

AD-751 918

A SIXTEEN-ELEMENT SBF ARRAY

Hermann W. Ehrenspeck, et al

Air Force Cambridge Research Laboratories  
L. G. Hanscom Field, Massachusetts

23 August 1972

DISTRIBUTED BY:

**NTIS**

National Technical Information Service  
U. S. DEPARTMENT OF COMMERCE  
5285 Port Royal Road, Springfield Va. 22151

AD 751918

AFCRL-72-0500  
23 AUGUST 1972  
PHYSICAL SCIENCES RESEARCH PAPERS, NO. 503



## AIR FORCE CAMBRIDGE RESEARCH LABORATORIES

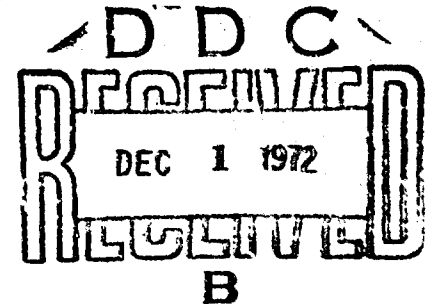
L. G. HANSCOM FIELD, BEDFORD, MASSACHUSETTS

### A Sixteen-Element SBF Array

HERMANN W. EHRENSPECK

JOHN A STROM

BEST  
AVAILABLE COPY



Approved for public release; distribution unlimited.

## AIR FORCE SYSTEMS COMMAND

### United States Air Force

Reproduced by  
NATIONAL TECHNICAL  
INFORMATION SERVICE

U.S. Department of Commerce  
Springfield VA 22151



ACCESSION for	
RTED	White Section <input checked="" type="checkbox"/>
CNC	Dark Section <input type="checkbox"/>
BRIEF CODES	
DISSEMINATION	
BY	
DISSEMINATION/AVAILABILITY CODES	
BRIEF CODES/RTED SPECIAL	
A	

Qualified requestors may obtain additional copies from the Defense Documentation Center. All others should apply to the National Technical Information Service.

Unclassified  
Security Classification

DOCUMENT CONTROL DATA - RLD		
(Security classification of title, body of abstract and indexing annotation must be entered when the overall report is classified)		
1. ORIGINATING ACTIVITY (Corporate author) Air Force Cambridge Research Laboratories (LZE) L. G. Hanscom Field Bedford, Massachusetts 01730		2a. REPORT SECURITY CLASSIFICATION Unclassified
		2b. GROUP
3. REPORT TITLE  A SIXTEEN-ELEMENT SBF ARRAY		
4. DESCRIPTIVE NOTES (Type of report and inclusive dates) Scientific. Interim.		
5. AUTHOR(S) (First name, middle initial, last name)  Hermann W. Ehrenspeck John A. Strom		
6. REPORT DATE 23 August 1972	7a. TOTAL NO. OF PAGES 51	7b. NO. OF REFS 9
8a. CONTRACT OR GRANT NO.		9a. ORIGINATOR'S REPORT NUMBER(S)  AFCRL-72-0500
a. PROJECT, TASK, WORK UNIT NOS. 4600-10-01		
c. DOD ELEMENT 62702F	9b. OTHER REPORT NO(S) (Any other numbers that may be assigned this report)	
d. DOD SUBELEMENT 681000	PSRP 508	
10. DISTRIBUTION STATEMENT  Approved for public release; distribution unlimited.		
11. SUPPLEMENTARY NOTES  TECH, OTHER		12. SPONSORING MILITARY ACTIVITY Air Force Cambridge Research Laboratories (LZE) L. G. Hanscom Field Bedford, Massachusetts 01730
13. ABSTRACT  Sixteen-element short-backfire arrays have been shown to yield maximum gains of approximately 25 dB. The influence of parameter variations on the array patterns and directivity has been experimentally determined by varying the frequency. A table of the normalized design parameters for an area efficiency of approximately 90 percent is given for construction purposes. All array dimensions are indicated in wavelengths so that each application can easily be scaled for any desired frequency range.		

DD FORM 1473  
1 NOV 65

Unclassified  
Security Classification

1a

**Unclassified**

**Security Classification**

KEY WORDS	LINK A		LINK B		LINK C	
	ROLE	WT	ROLE	WT	ROLE	WT
SBF array						
Short-backfire antenna						
Antenna array design						
Antenna performance						

Unclassified  
Security Classification

AFCRL-72-0500  
23 AUGUST 1972  
PHYSICAL SCIENCES RESEARCH PAPERS, NO. 508



MICROWAVE PHYSICS LABORATORY      PROJECT 4600

## **AIR FORCE CAMBRIDGE RESEARCH LABORATORIES**

L. G. HANSCOM FIELD, BEDFORD, MASSACHUSETTS

# **A Sixteen-Element SBF Array**

HERMANN W. EHRENSPECK

JOHN A STROM

Approved for public release; distribution unlimited.

**AIR FORCE SYSTEMS COMMAND**  
**United States Air Force**



ic

## Abstract

Sixteen-element short-backfire arrays have been shown to yield maximum gains of approximately 25 dB. The influence of parameter variations on the array patterns and directivity has been experimentally determined by varying the frequency. A table of the normalized design parameters for an array efficiency of approximately 90 percent is given for construction purposes. All array dimensions are indicated in wavelengths so that each application can easily be scaled for any desired frequency range.

Preceding page blank

## Contents

1.	INTRODUCTION	1
2.	THE SIXTEEN-ELEMENT SBF ARRAY	2
2.1	Description of Array	2
2.2	Dimensions of Array	3
3.	EXPERIMENTAL RESULTS	4
3.1	Sum Patterns of Array as Function of Frequency	4
3.2	Sum Patterns of Array at Design Frequency (3.0 GHz)	6
3.3	Difference Patterns of Array as Function of Frequency	6
3.4	Difference Patterns of Array at Design Frequency (3.0 GHz)	8
3.5	Array Directivity as Function of Frequency	8
4.	COMMENTS	9
	REFERENCES	41
	APPENDIX A. Description of the Slot Dipoles Used as Feed Elements in the 3-GHz Array Models	43

## Illustrations

1.	Sketch of Sixteen-Element SBF Array	3
2.	Sketch of Cross-Sectional Side View of One of the Non-Corner Outer SBF Elements	3



## Illustrations

3.	Photograph of Experimental Sixteen-Element SBF Array	5
4.	Photograph of Coaxial Cable Network for Experimental Sixteen-Element SBF Array	5
5.	Experimental Curves of Half-Power Beamwidth and First Sidelobe Level of the Sixteen-Element SBF Array as a Function of Frequency	7
6.	Radiation Pattern of Sixteen-Element SBF Array at $f = 2.7$ GHz (E plane)	11
7.	Radiation Pattern of Sixteen-Element SBF Array at $f = 2.8$ GHz (E plane)	12
8.	Radiation Pattern of Sixteen-Element SBF Array at $f = 2.9$ GHz (E plane)	13
9.	Radiation Pattern of Sixteen-Element SBF Array at $f = 3.0$ GHz (E plane)	14
10.	Radiation Pattern of Sixteen-Element SBF Array at $f = 3.1$ GHz (E plane)	15
11.	Radiation Pattern of Sixteen-Element SBF Array at $f = 3.2$ GHz (E plane)	16
12.	Radiation Pattern of Sixteen-Element SBF Array at $f = 3.3$ GHz (E plane)	17
13.	Radiation Pattern of Sixteen-Element SBF Array at $f = 2.7$ GHz (H plane)	18
14.	Radiation Pattern of Sixteen-Element SBF Array at $f = 2.8$ GHz (H plane)	19
15.	Radiation Pattern of Sixteen-Element SBF Array at $f = 2.9$ GHz (H plane)	20
16.	Radiation Pattern of Sixteen-Element SBF Array at $f = 3.0$ GHz (H plane)	21
17.	Radiation Pattern of Sixteen-Element SBF Array at $f = 3.1$ GHz (H plane)	22
18.	Radiation Pattern of Sixteen-Element SBF Array at $f = 3.2$ GHz (H plane)	23
19.	Radiation Pattern of Sixteen-Element SBF Array at $f = 3.3$ GHz (H plane)	24
20.	Difference Pattern of Sixteen-Element SBF Array at $f = 2.7$ GHz (E plane)	25
21.	Difference Pattern of Sixteen-Element SBF Array at $f = 2.8$ GHz (E plane)	26
22.	Difference Pattern of Sixteen-Element SBF Array at $f = 2.9$ GHz (E plane)	27
23.	Difference Pattern of Sixteen-Element SBF Array at $f = 3.0$ GHz (E plane)	28
24.	Difference Pattern of Sixteen-Element SBF Array at $f = 3.1$ GHz (E plane)	29

## Illustrations

25.	Difference Pattern of Sixteen-Element SBF Array at $f = 3.2$ GHz (E plane)	30
26.	Difference Pattern of Sixteen-Element SBF Array at $f = 3.3$ GHz (E plane)	31
27.	Difference Pattern of Sixteen-Element SBF Array at $f = 2.7$ GHz (H plane)	32
28.	Difference Pattern of Sixteen-Element SBF Array at $f = 2.8$ GHz (H plane)	33
29.	Difference Pattern of Sixteen-Element SBF Array at $f = 2.9$ GHz (H plane)	34
30.	Difference Pattern of Sixteen-Element SBF Array at $f = 3.0$ GHz (H plane)	35
31.	Difference Pattern of Sixteen-Element SBF Array at $f = 3.1$ GHz (H plane)	36
32.	Difference Pattern of Sixteen-Element SBF Array at $f = 3.2$ GHz (H plane)	37
33.	Difference Pattern of Sixteen-Element SBF Array at $f = 3.3$ GHz (H plane)	38
34.	Experimental Curve of Directivity of the Sixteen-Element SBF Array as a Function of Frequency	39
A1.	Sketch of Cross-Sectional View of Slot Dipole and Matching Section of SBF Element	44
A2.	Smith Chart Plot of Matching Curve of the SBF Element in a SBF Array	44

## Tables

1.	Array Dimensions for $f_0 = 3.0$ GHz	4
2.	Array Dimensions for $f = 2.9$ GHz	9

## A Sixteen-Element SBF Array

### 1. INTRODUCTION

In earlier reports of our series on short-backfire (SBF) antennas and arrays, we introduced the concept of the SBF element (Ehrenspeck, 1965, 1969, 1970) as a new type of array element for high-gain antennas (Ehrenspeck and Strom, 1971a). We also discussed two-, four-, and eight-element SBF arrays in the gain range of 17 to 22 dB (Ehrenspeck and Strom, 1971b), and described detailed design data for a four-element 20-dB SBF array optimized for those special pattern characteristics that result in highest array gain, lowest side- and backlobe levels, equal half-power beamwidths, or equal beam shapes, in the E and H planes (Ehrenspeck and Strom, 1971c). As a continuation in this series, the present report deals with an experimental study of a sixteen-element SBF array that reaches a gain of 25 dB.

Contemporary antenna arrays with gains of 20 to 25 dB are usually designed with many closely spaced slot or dipole elements in front of a common reflector. The properly tapered illumination of the reflector area is provided by adjusting the amplitude and phase of each of the elements by attenuation and phase-shift in the input-output circuitry. This practice introduces losses and thermal noise and reduces the directive gain of the array. One of the largest dipole arrays in use for satellite tracking yields a gain of 22 dB with 48 dipoles (Oettl and

---

(Received for publication 22 August 1972)

Thomanek, 1968). If a gain of 25 dB is desired, the number of dipole array elements would have to be increased to more than 100. The use of SBF elements, however, reduces the number of feed elements to 16, since any SBF element will replace as many as 6 dipoles. The amplitude and phase adjustment devices can be completely eliminated, resulting in a markedly increased array efficiency.

The experimental work described in this report includes measurements of the radiation patterns and antenna directivities of a typical 16-element SBF array. Since such high-gain arrays are likely to be used for communications and telemetry as well as for monopulse tracking, the sum and difference patterns are presented for both the E and H planes.

The experimental array model was designed to perform optimally at a frequency of 3.0 GHz, which is the same as that used for antenna models in our earlier reports (Ehrenspeck and Strom, 1971a, b, c).

## 2. THE SIXTEEN-ELEMENT SBF ARRAY

### 2.1 Description of Array

Figure 1 shows a front view of a typical sixteen-element SBF array. It consists of sixteen separately fed SBF elements backed by a common planar squarish reflector M of side length  $D_M$ , with each corner curved at a radius  $r$  ( $r = D_M/5$ ) from the element proximal to it. Reflector M is bounded by a rim B of width  $W_B$ . The reflector disks of the SBF elements are denoted R. All SBF elements are equispaced center-to-center a distance  $S_E (=r)$ . The structure is symmetric with respect to its diagonal as well as its x and y axes. Sum patterns can be obtained by rotating the array around any of the three axes; for difference patterns, however, only the x or y axis can be used. The patterns relevant to this study were measured by rotating the array about the x and y axes. Figure 2 is an enlarged cross-sectional side view of one of the non-corner SBF elements of the upper element row in Figure 1. The spacing between reflector M and the feeds F, and between reflector M and disk reflector R, are denoted  $S_F$  and  $S_R$ , respectively. Feeds F are slotted dipoles, but crossed dipoles can be substituted for circular polarization response or monopulse tracking in azimuth and elevation. Rods Q, which support the reflector disks R, are insulated in this particular application. For other feed structures, for example, symmetrically fed dipoles or equivalent radiators, metal rods would suffice. Although SBF elements have the same dimensions, their specific contributions to the array pattern are different because they depend on their location in respect to their neighboring elements and the rim dimensions. In the described array model, as in models of earlier reports, the

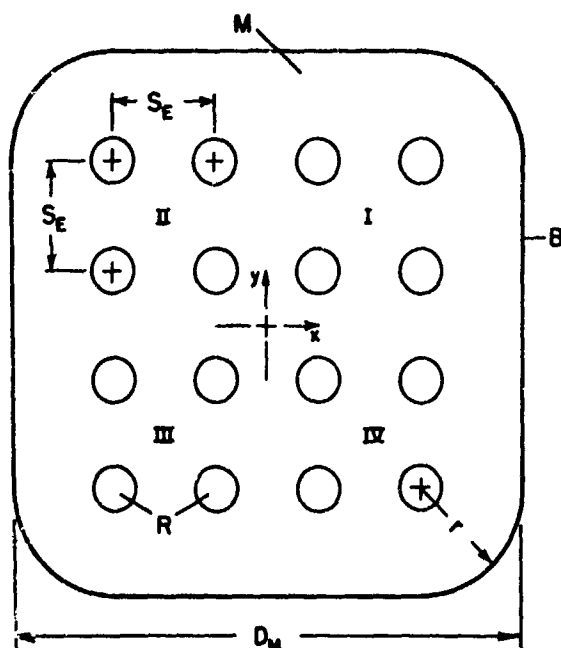


Figure 1. Sketch of Sixteen-Element SBF Array

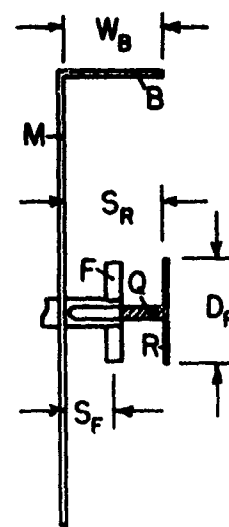


Figure 2. Sketch of Cross-Sectional Side View of One of the Non-Corner Outer SBF Elements

rim depth  $W_B$  is shown equal to  $S_H$ . For flushmounted or weatherproof array applications, this configuration offers the advantage that the entire structure can be easily covered by a dielectric plate. Reflector M consists of the four cartesian quadrants I, II, III, and IV, each of which contains four SBF elements. This arrangement provides operational symmetry for the sum and difference patterns in the E as well as in the H, plane of the array.

## 2.2 Dimensions of Array

The dimensions of the experimental sixteen-element SBF array model were chosen consistent with those of our previous SBF array models except for the spacing  $S_E$  of the elements. Earlier investigations of a four-element SBF array had indicated a further increase in directivity for a slightly wider element spacing. The first sidelobes were still lower than -14 to -16 dB in the E- and H-plane patterns (Ehrenspeck and Strom, 1971c). Therefore, the same value of  $S_E$  was chosen for the newly developed sixteen-element SBF array described in this report. The array parameters referred to the design frequency  $f_0 = 3.0$  GHz ( $\lambda_0 = 10.0$  cm) are listed in Table 1.

Table 1. Array Dimensions for  $f_c = 3.0$  GHz

---



---

$D_M$	$= 5.63 \lambda_o$
$r$	$= 1.13 \lambda_o$
$D_R$	$= 0.50 \lambda_o$
$S_R$	$= 0.50 \lambda_o$
$S_F$	$= 0.25 \lambda_o$
$W_B$	$= 0.50 \lambda_o$
$M$	$= 30.55 \lambda_o^2$ (area)

---

Photographs of the described experimental array model and its input circuitry are shown in Figures 3 and 4, respectively. The cabling consists of phase-stable 50-ohm coaxial sections (Times Wire and Cable Type SF-42), which are adjusted to equal electrical length, and of balanced fourport power dividers (Omni Spectra, Type OS 20244). Each of the quadrants I, II, III, and IV of the array, together with a divider, forms a unit. For the sum patterns, cables of equal electrical length connect the four quadrant units with a fifth fourport power divider, whose output is the sum voltage of all sixteen elements. For obtaining the difference patterns in azimuth or elevation, the fifth power divider is replaced by two twoport dividers (Omni Spectra Type OS 20224) and a coaxial magic tee (hybrid) providing the necessary  $180^\circ$  phase shift for the pattern minimum in the center axis of the array. For determining the azimuthal angles, the quadrant units I + IV and II + III—and for the elevation angles, the quadrant units I + II and III + IV—are connected with the twoport dividers, and all dipoles rotated into the direction of polarization. This procedure must be followed because crossed dipoles are difficult to construct for the GHz frequency range of our experimental slotted-dipole array models. This method of measuring the E- and H-plane patterns of the array is justifiable since for applications at lower frequencies, the coupling between the two members of a carefully designed crossed dipole can always be made better than 30 dB.

### 3. EXPERIMENTAL RESULTS

#### 3.1 Sum Patterns of Array as Function of Frequency

The experimental investigations of the sixteen-element SBF array model included the measurement of the sum and difference patterns and directivities over the frequency range 2.2 to 3.6 GHz. All measurements were performed in an

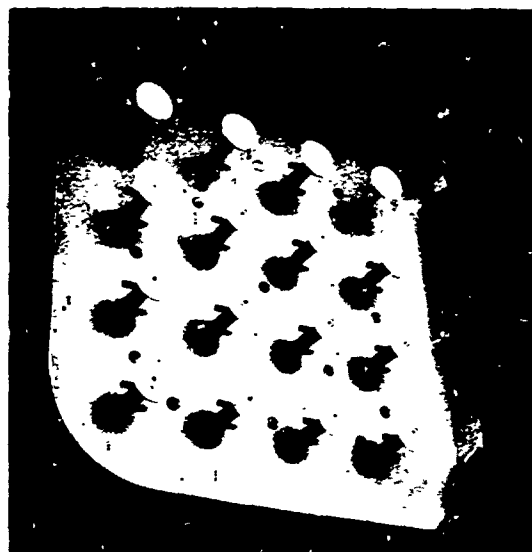


Figure 3. Photograph of Experimental Sixteen-Element SBF Array

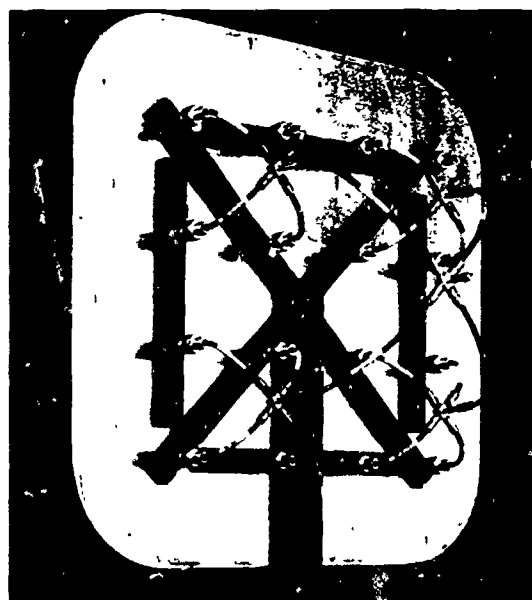


Figure 4. Photograph of Coaxial Cable Network for Experimental Sixteen-Element SBF Array

anechoic test facility. In all patterns shown in this report, the energy level of the main beam was always adjusted to the same maximum amplitude. The array directivities were measured according to the pattern integration technique described by Fulmer and Moseley (1960).

Figure 5 shows (a) the half-power beamwidth and (b) the level of the first sidelobe as a function of frequency in increments of 0.1 GHz. Since the first sidelobe was to be limited to approximately -13 dB the useful frequency range was limited to 2.7 to 3.3 GHz, as indicated by the two perpendicular lines. Figures 6 to 12 present the E-plane and Figures 13 to 19 the H-plane patterns over this frequency range. It will be noted that the beamwidth varies from  $12.5^\circ$  to  $10.5^\circ$  in the E plane, and from  $11.5^\circ$  to  $10.5^\circ$  in the H plane. The pattern bandwidth of the array is determined by the allowable sidelobe level. It is approximately  $\pm 10$  percent for sidelobe level limitations of -13 to -14 dB, and is remarkably wider if higher sidelobes can be tolerated. For some frequencies below 2.7 GHz and above 3.3 GHz, additional sidelobes appear at angles approximately  $60^\circ$  to  $70^\circ$  off the axis. These must be taken into account if the array has to be used for a frequency range wider than  $\pm 10$  percent. Such patterns are, however, still acceptable for many applications.

### 3.2 Sum Patterns of Array at Design Frequency (3.0 GHz)

The array patterns for the design frequency (3.0 GHz) are presented in Figures 9 and 16 for the E and H planes, respectively. The half-power beamwidths are  $11^\circ$  and  $10.5^\circ$ , and the first sidelobes at at -13.5 dB and -14.8 dB, respectively. All other lobes are below these values. At angles of  $\pm 90^\circ$  from the axis, all lobes decrease to -30 dB and the backlobe is measured at about -40 dB. The directivity calculated from an improved gain beamwidth product equation (Stegen, 1964) is 25.1 dB. This value is in good agreement with the 24.9-dB directivity measurement obtained by pattern integration and corresponds to an area efficiency of 80 percent (referred to the area of reflector M).

### 3.3 Difference Patterns of Array as Function of Frequency

To show the tracking capability of the array, the difference patterns are presented in Figures 20 to 26 for the E plane and in Figures 27 to 33 for the H plane. The level of the mainlobes has always been adjusted to the same reference level, which allows a dynamic range of 30 dB. All patterns show the sharp minima that are necessary for accurate tracking in both azimuth and elevation angles. At the design frequency, sidelobe levels of approximately -16 dB are obtained. At a frequency approximately 3 percent lower, the sidelobe level decreases to nearly -20 dB. Mostly all further-out lobes in the E- and H-plane patterns decrease to at least -30 dB.



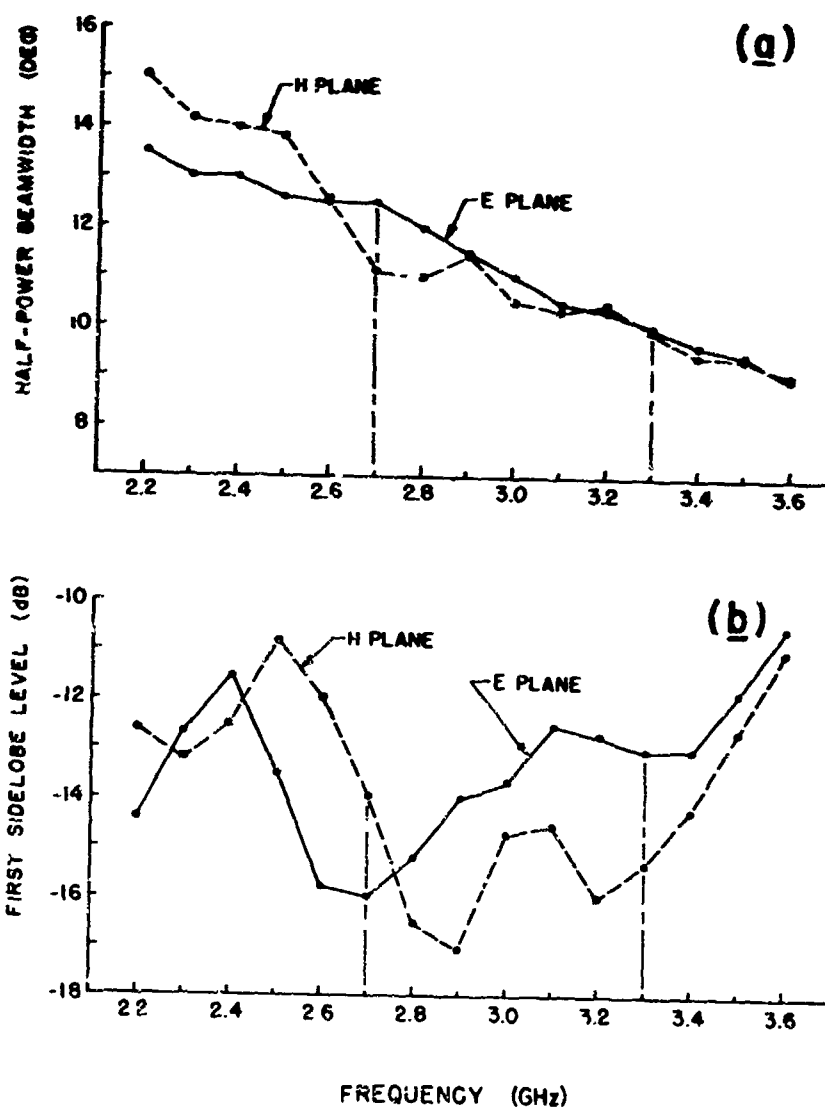


Figure 5. Experimental Curves of (a) Half-Power Beamwidth, and (b) First Sidelobe Level of the Sixteen-Element SBF Array as a Function of Frequency

### 3.4 Difference Patterns of Array at Design Frequency (3.0 GHz)

The array patterns for the design frequency (3.0 GHz) are presented in Figures 23 and 30. They indicate sidelobes of -17.5 dB and 15.5 dB in the E and H planes, respectively. All other sidelobes are lower than -21 dB and far below -30 dB in the angular range from  $90^\circ$  to  $270^\circ$ . The minima are far below -30 dB.

### 3.5 Array Directivity as Function of Frequency

The array directivities were measured by pattern integration over the same frequency range as the patterns. The results are shown in Figure 34. A directivity of almost 25 dB was achieved at the design frequency. Slightly greater values, to a maximum of 25.5 dB, were measured at a frequency approximately 10 percent higher. If, however, the directivity values are referred to the reflector area and the results discussed in terms of array efficiency, the picture is different.

The array directivity can be calculated as  $D = e (4\pi A/\lambda^2)$ , where  $A$  is the reflector area expressed in  $\lambda^2$ , and  $e$  is the aperture illumination efficiency defined as the ratio of the measured directivity to the directivity obtained with uniform aperture illumination. The efficiency reaches 100 percent if the total reflector area of the array is uniformly illuminated. Calculated array directivity curves for values of  $e$  between 65 and 100 percent as functions of frequency are plotted in Figure 34. It is evident that the array has an area efficiency of approximately 80 percent at the design frequency (3.0 GHz) and at the frequency yielding the highest directivity (approximately 3.3 GHz). These high efficiency values are consistent with the earlier measurements on SBF arrays of fewer elements (see Ehrenspeck and Strom, 1971 a, b, c).

Of special interest is the directivity value measured for 2.9 GHz, which shows an area efficiency of nearly 90 percent. In checking the corresponding sum and difference patterns of Figures 8, 15, 22, and 29, it was found that they indicate an even better overall performance than those for the design frequency. From these results a new table of optimum array parameters of a sixteen-element SBF array whose area efficiency is approximately 90 percent can be developed by scaling the dimensions of Table 1 for the 2.9-GHz frequency. The resulting dimensions are listed in Table 2. The radiation patterns of this array are those shown in Figures 8, 15, 22, and 29. The directivity of the optimized SBF array is 25 dB, or, 1.4 dB greater than that of a conventional array having an aperture illumination efficiency of 65 percent, for the same reflector area and approximately the same pattern quality.

Table 2. Array Dimensions for  $f = 2.9$  GHz

---



---

$D_M$	$= 5.44 \lambda$
$r$	$= 1.09 \lambda$
$D_R$	$= 0.48 \lambda$
$S_R$	$= 0.48 \lambda$
$S_F$	$= 0.24 \lambda$
$W_B$	$= 0.48 \lambda$
$M$	$= 28.55 \lambda^2$ (area)

---

#### 4. COMMENTS

The sixteen-element SBF array has excellent radiation patterns and directivity characteristics for antenna applications in the gain range near 25 dB. Both the sum- and difference-pattern bandwidths are sufficient for most uses. The impedance bandwidth could not be investigated because of the relatively high frequency for which the described array model was designed. This problem has, however, been solved for applications at lower frequency ranges such as those used in the Tactical Satellite Communication System (TACSATCOM) and in a four-element SBF array developed for the U. S. Naval Underwater Sound Laboratory (see Ehrenspeck and Strom, 1971c). Both antennas use sleeve-type crossed dipole feeds that provide excellent impedance-matching in the 240- to 315-MHz frequency range.

The reflector of the experimental 3-GHz model array of Figure 1 was fabricated from sheet aluminum. If weight and wind resistance are considerations, such as for array structures for VHF and UHF frequencies, expanded aluminum or similar materials can be used. The mesh openings of such materials have to be smaller than 0.1 wavelength of the highest operating frequency.

The extremely high aperture illumination efficiency of the array results in a markedly decreased reflector size. The reflector area of the described SBF array is only approximately 0.7 times that of conventional 25-dB arrays, which usually yield the same pattern characteristics with illumination efficiencies of approximately 65 percent.

In general, the combination of good-quality sum and difference patterns and high directivity renders the sixteen-element SBF array an attractive antenna that competes very well with contemporary multielement arrays. For approximately the same performance, these other multielement arrays would need more

than 100 separately fed dipole elements. The markedly smaller reflector size and lower number of feeds required by the sixteen-element SBF array reduces construction costs and line losses while improving the reliability of operation.

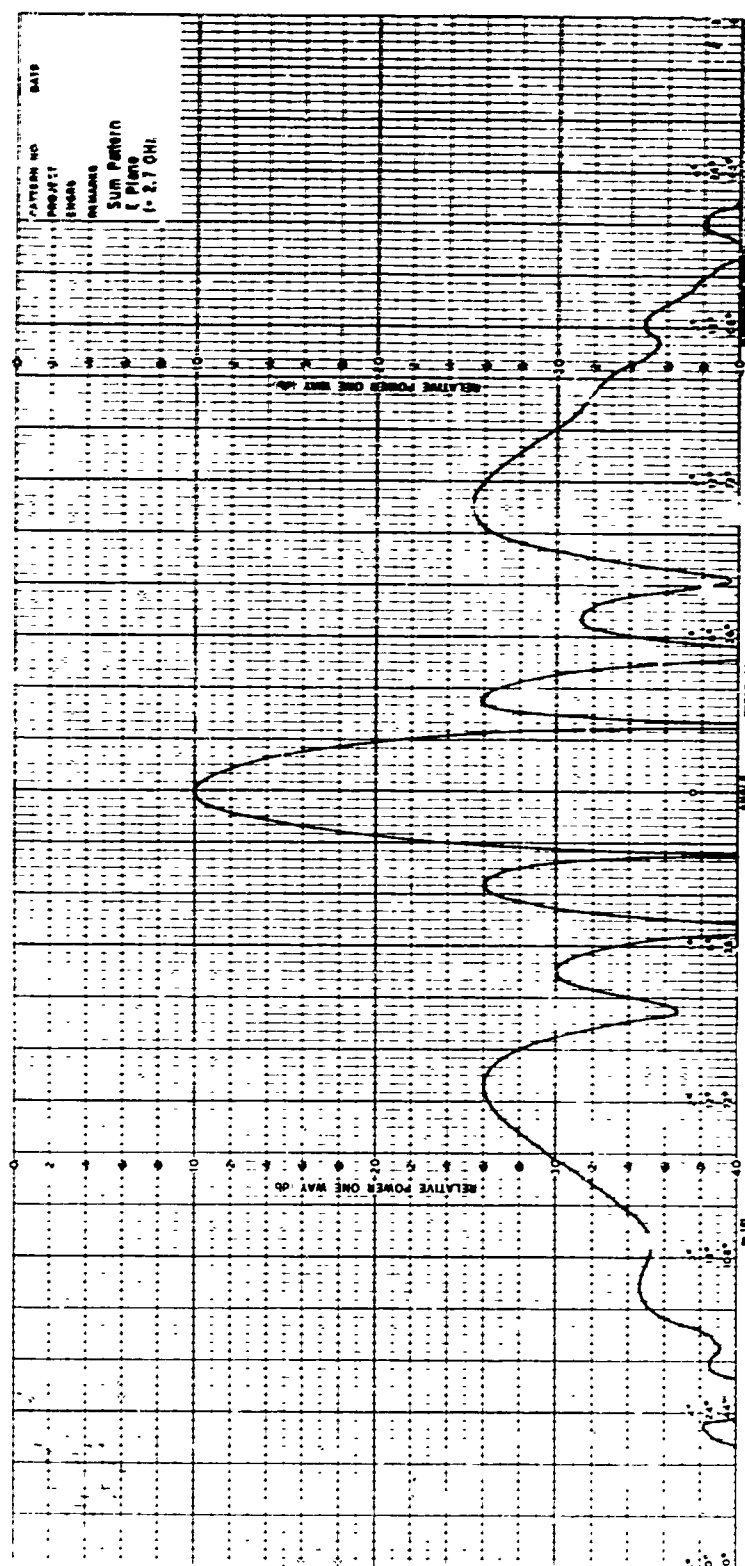


Figure 6. Radiation Pattern of Sixteen-Element SBF Array at  $f = 2.7$  GHz (E plane)

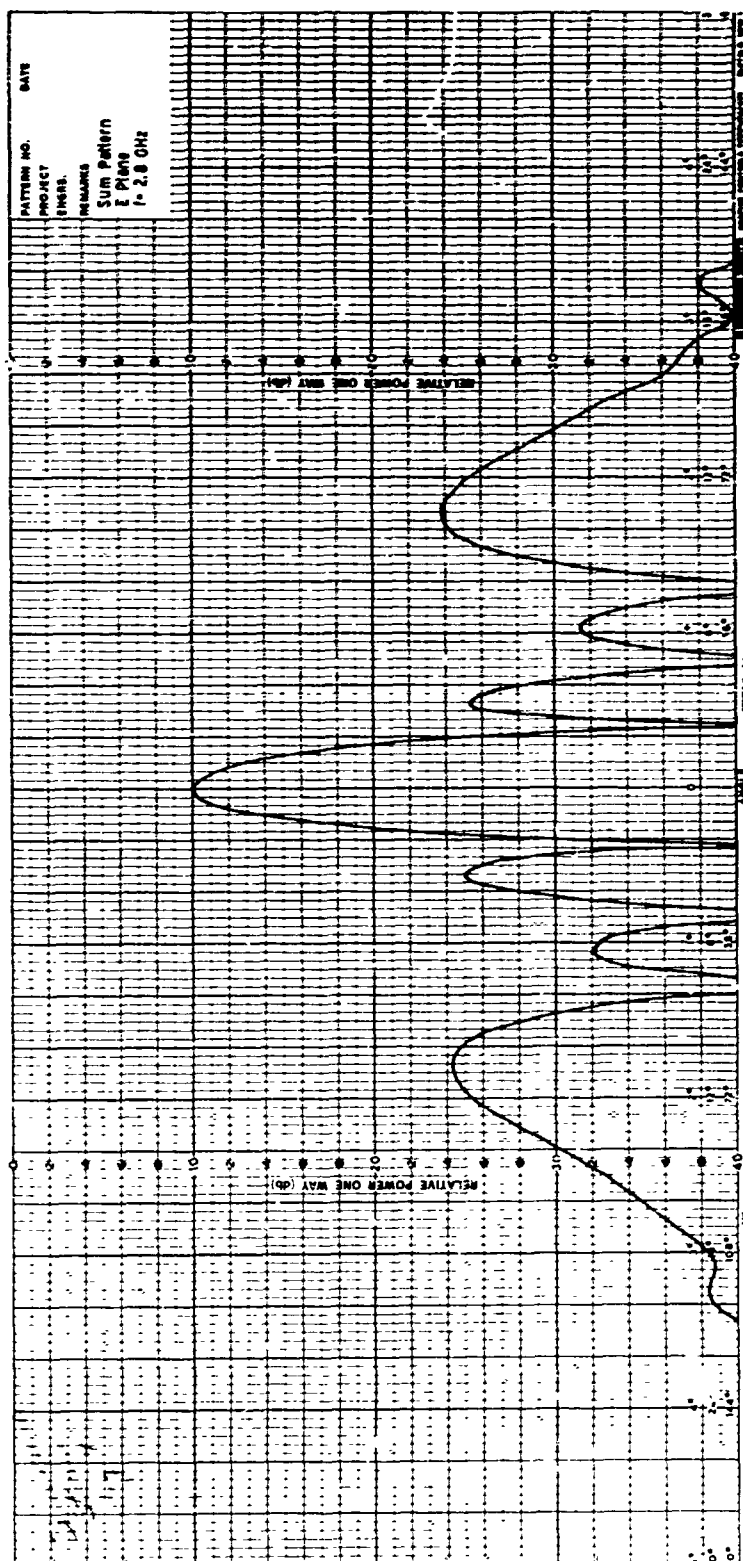


Figure 7. Radiation Pattern of Sixteen-Element SBF Array at  $f = 2.8$  GHz (E plane)

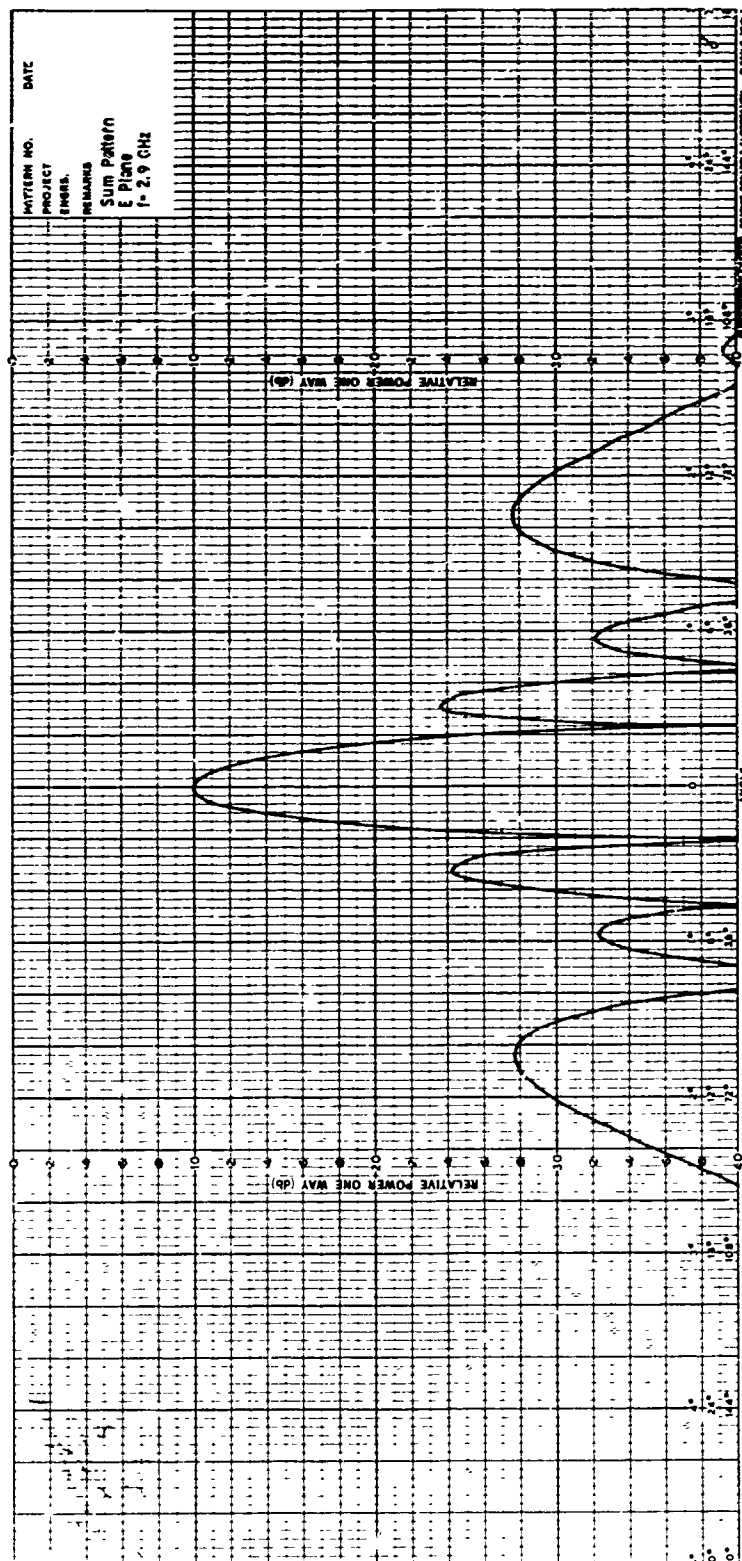
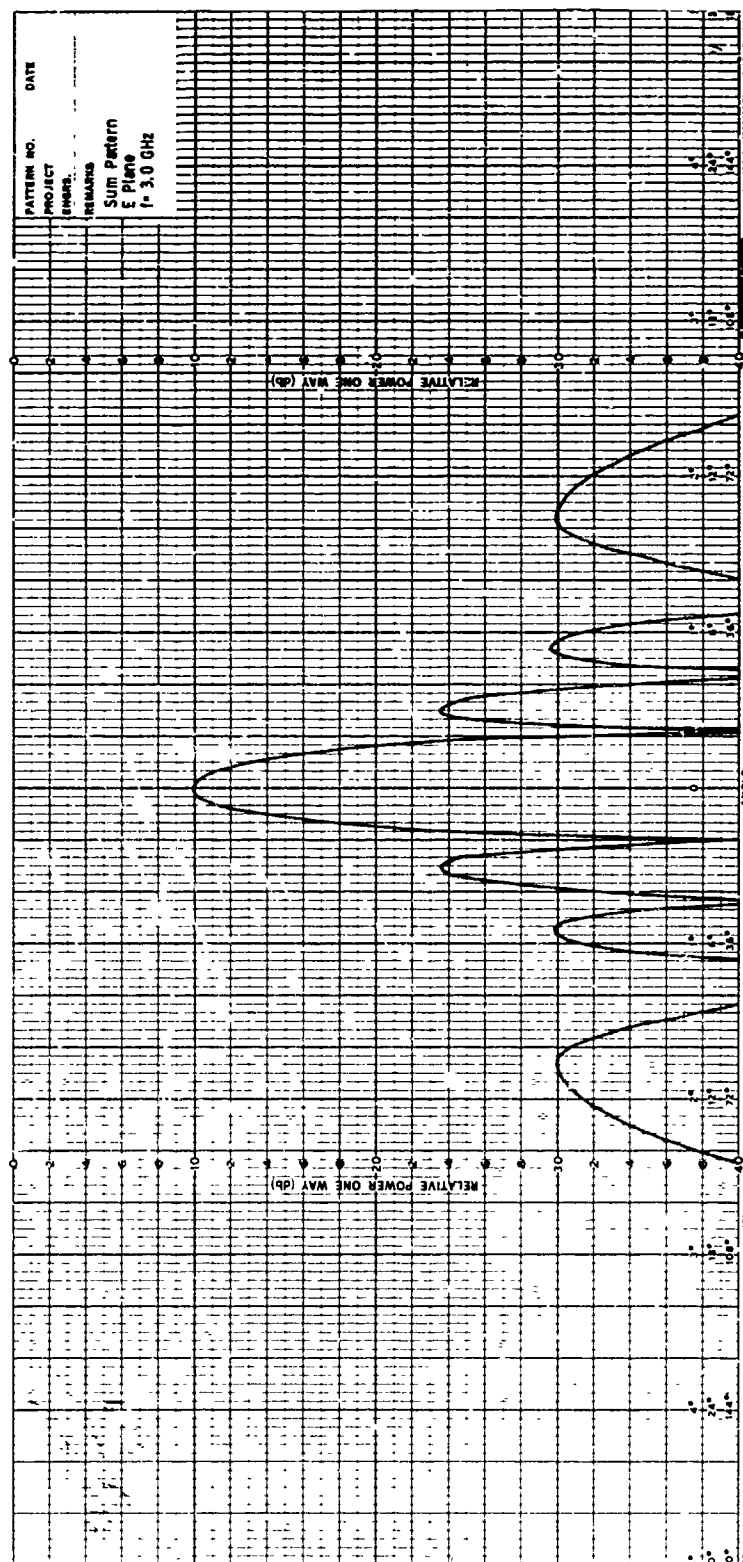


Figure 8. Radiation Pattern of Sixteen-Element SBF Array at  $f = 2.9 \text{ GHz}$  (E plane)





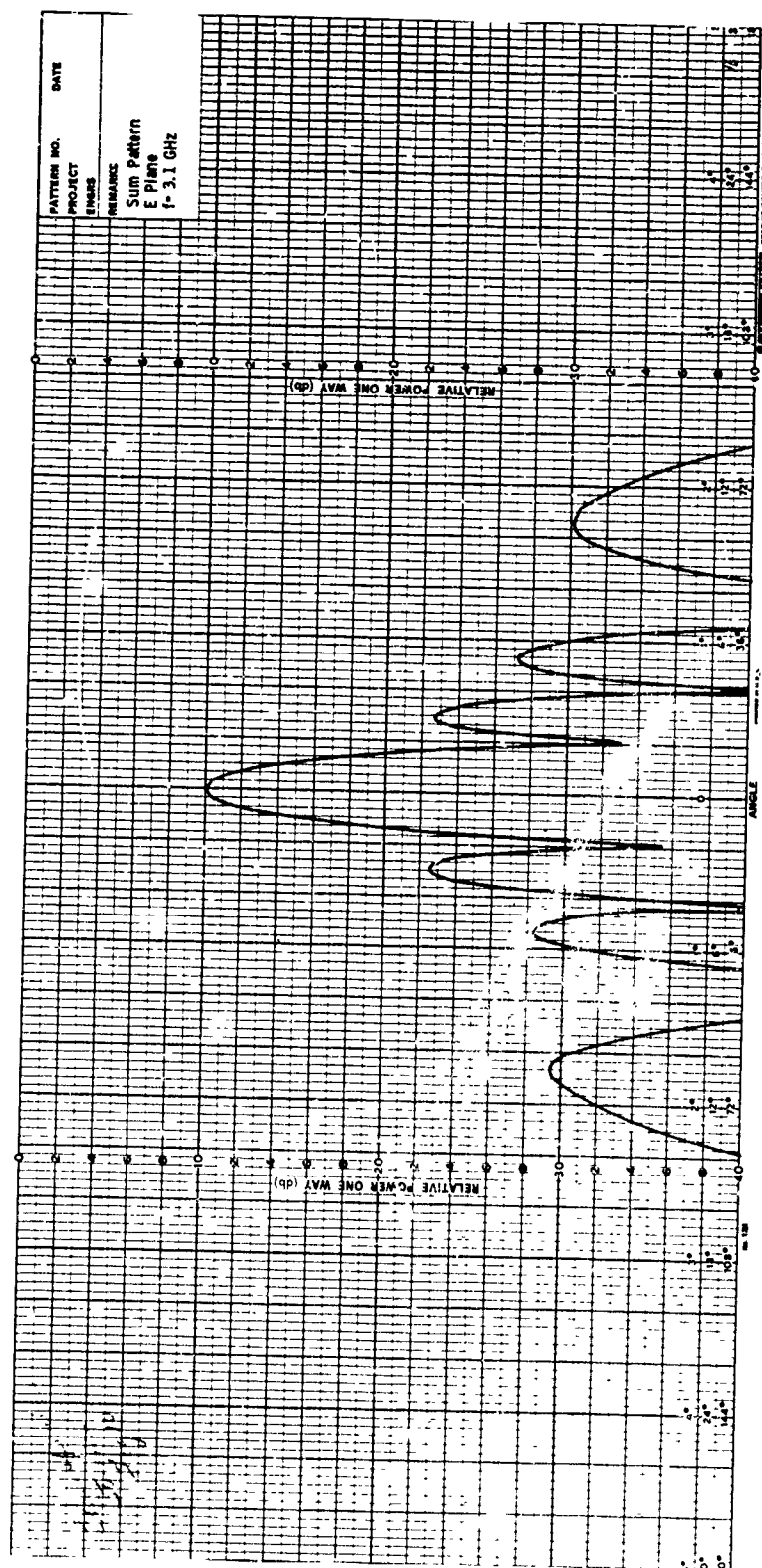


Figure 10. Radiation Pattern of Sixteen-Element SBF Array at  $f = 3.1$  GHz (E plane)

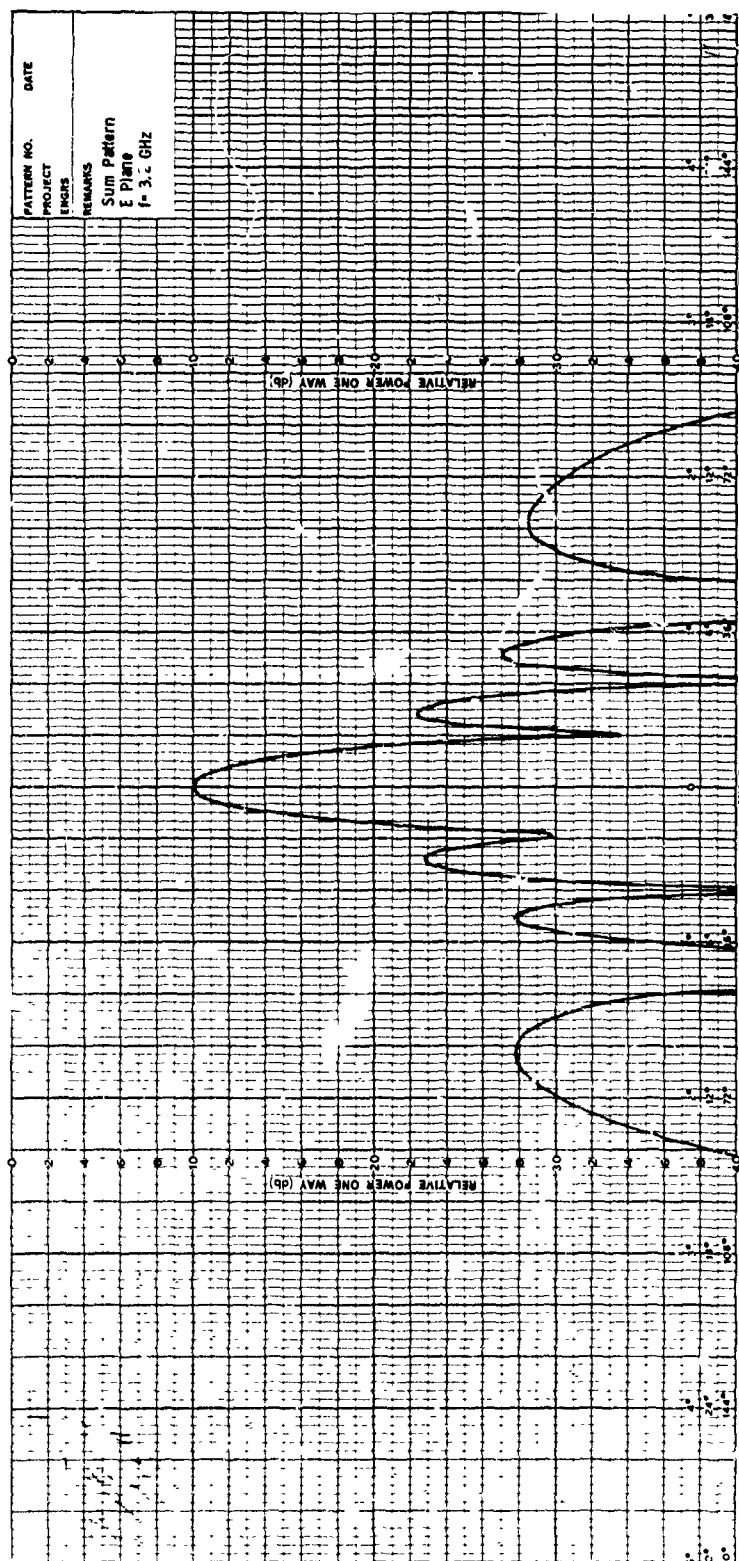


Figure 11. Radiation Pattern of Sixteen-Element SBF Array at  $f = 3.2$  GHz (E plane)

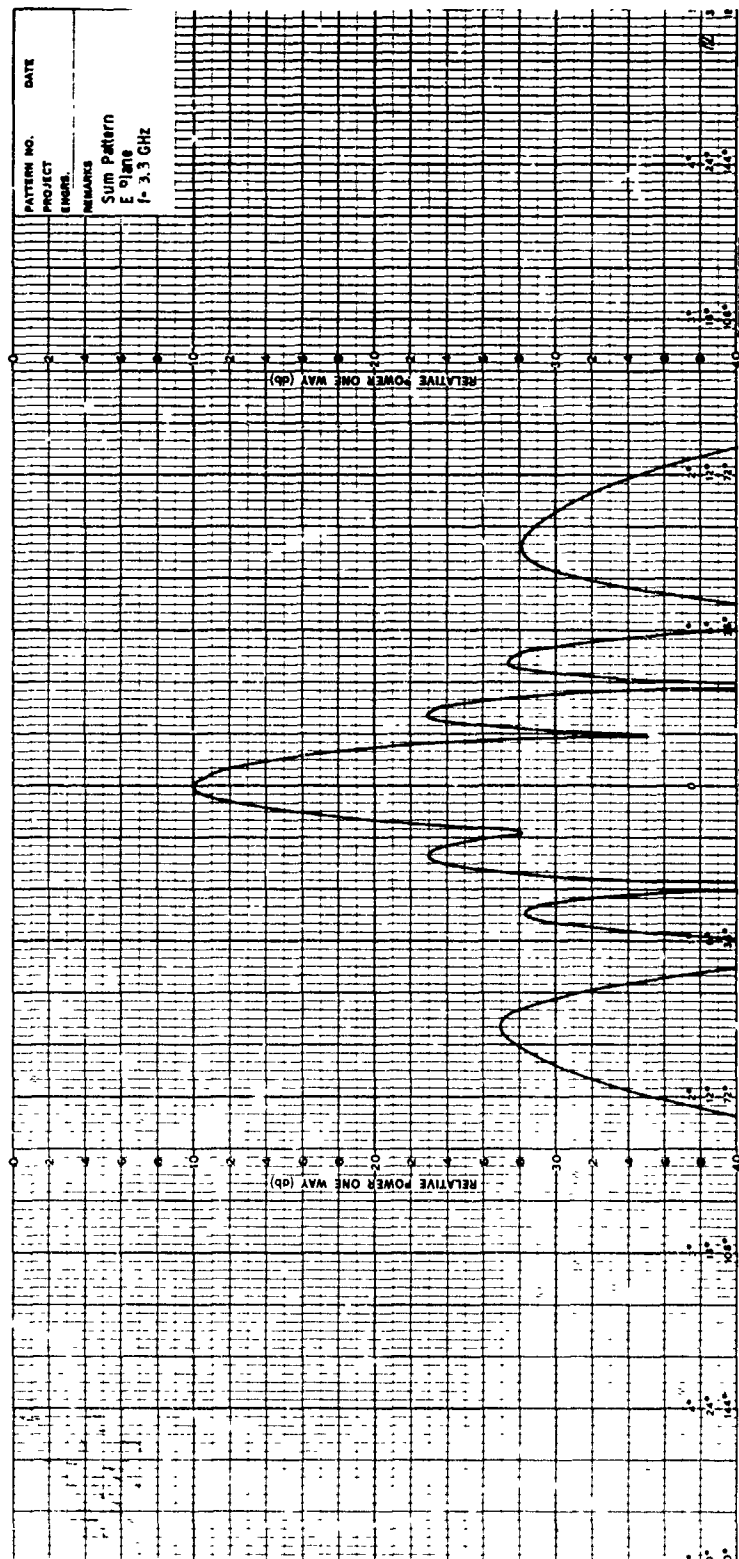


Figure 12. Radiation Pattern of Sixteen-Element SBF Array at  $f = 3.3$  GHz (E plane)

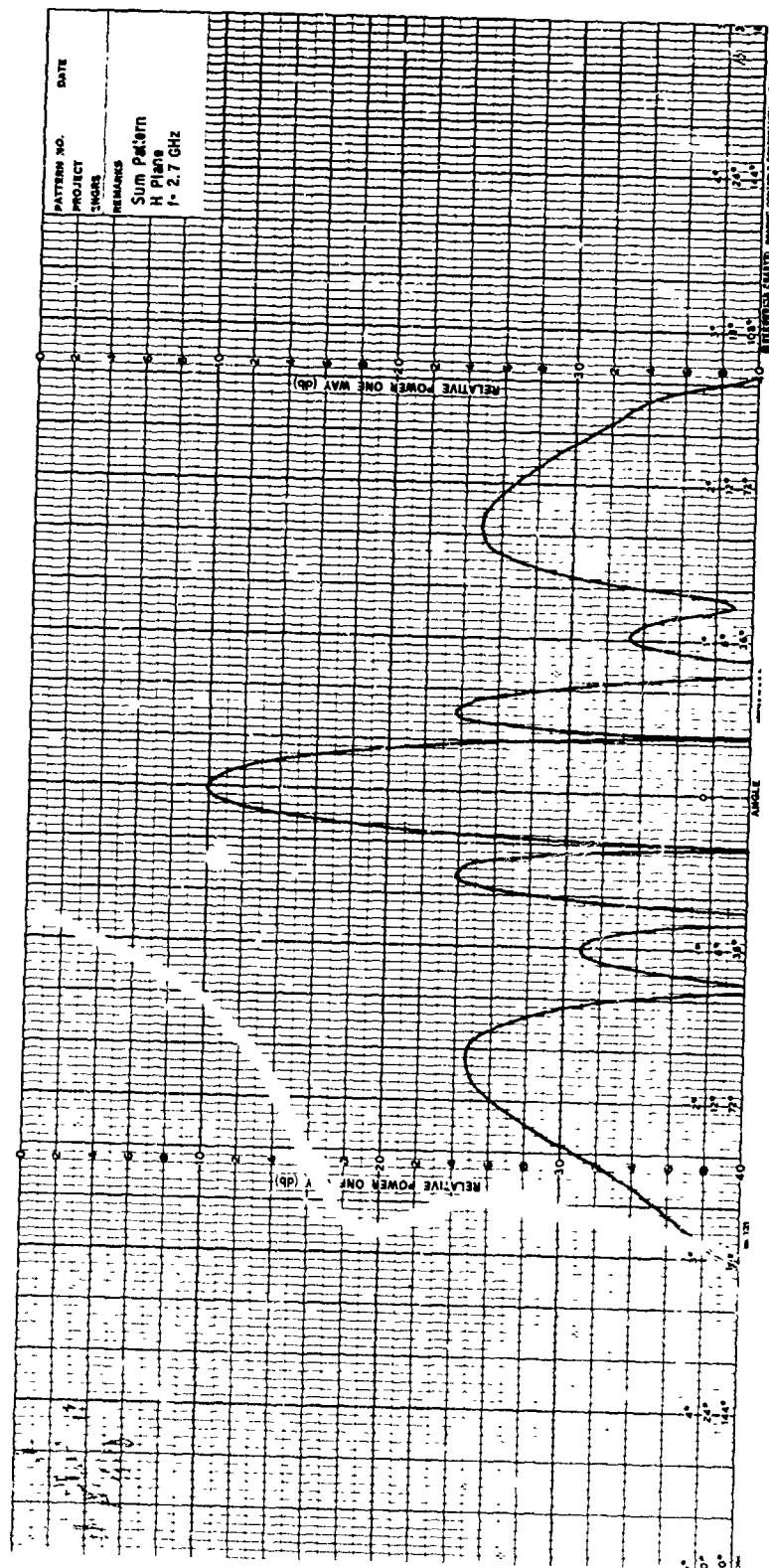


Figure 13. Radiation Pattern of Sixteen-Element SBF Array at  $f = 2.7$  GHz (H plane)

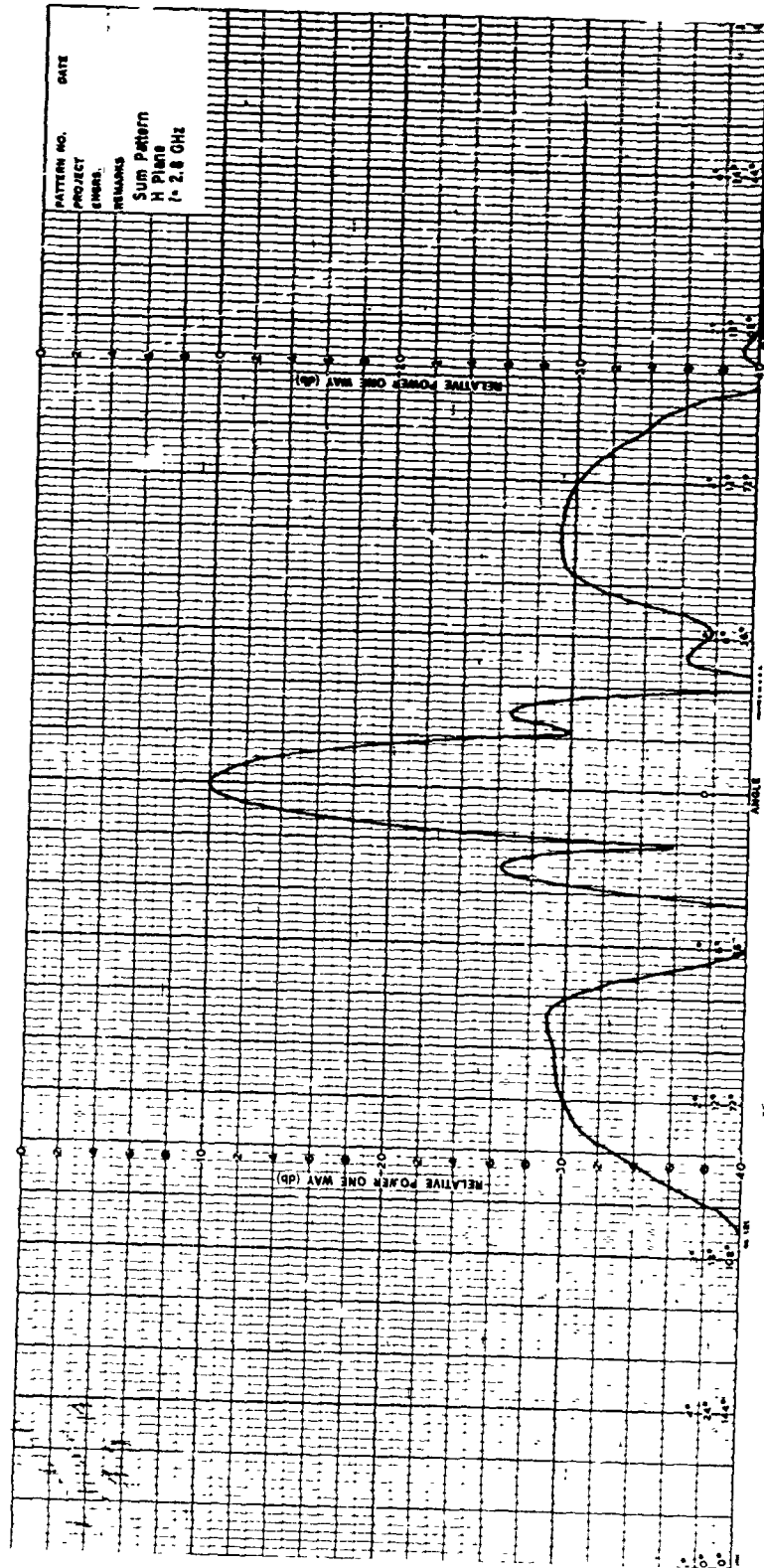


Figure 14. Radiation Pattern of Sixteen-Element SBF Array at  $f = 2.8 \text{ GHz}$  (H plane)

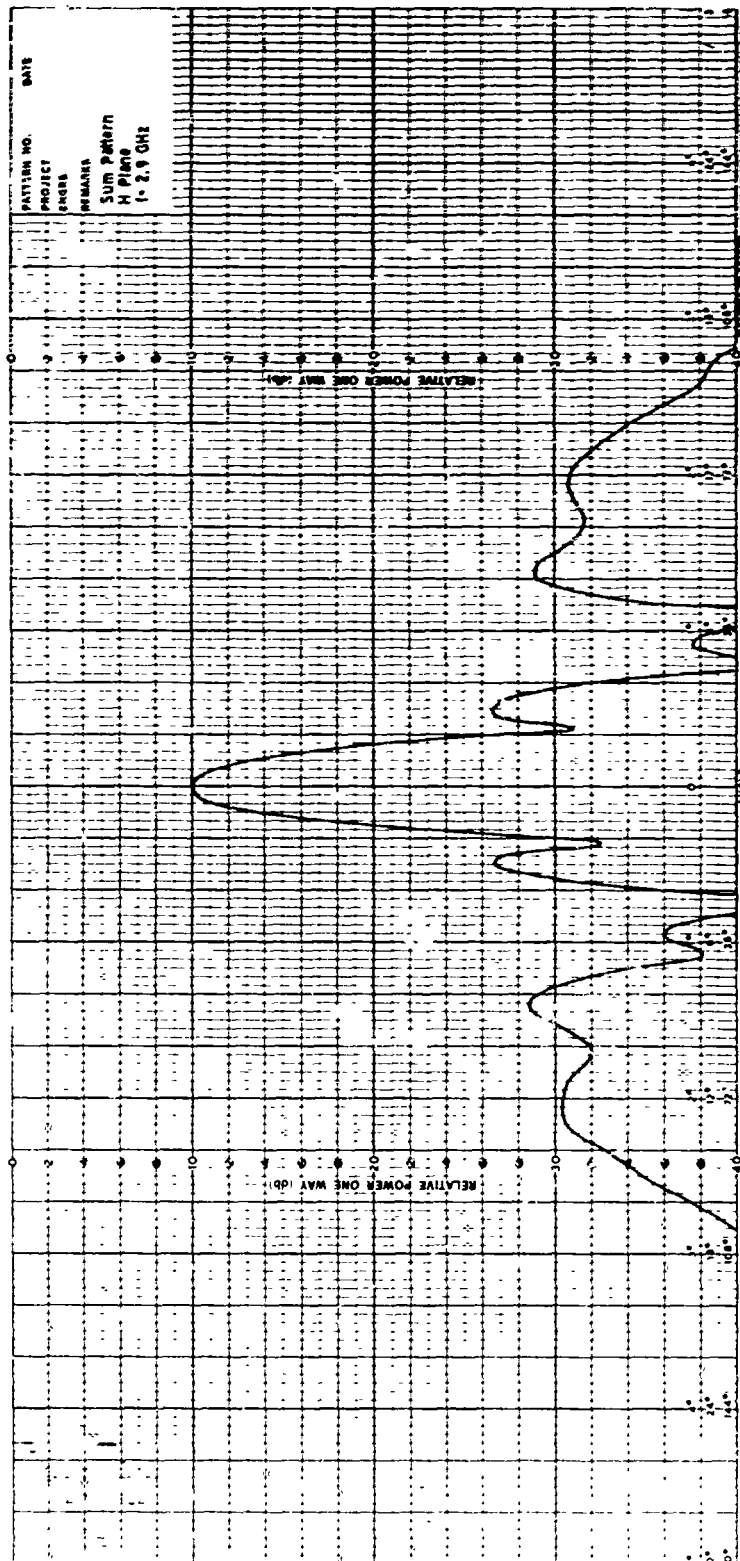


Figure 15. Radiation Pattern of Sixteen-Element SBF Array at  $f = 2.9$  GHz (H plane)

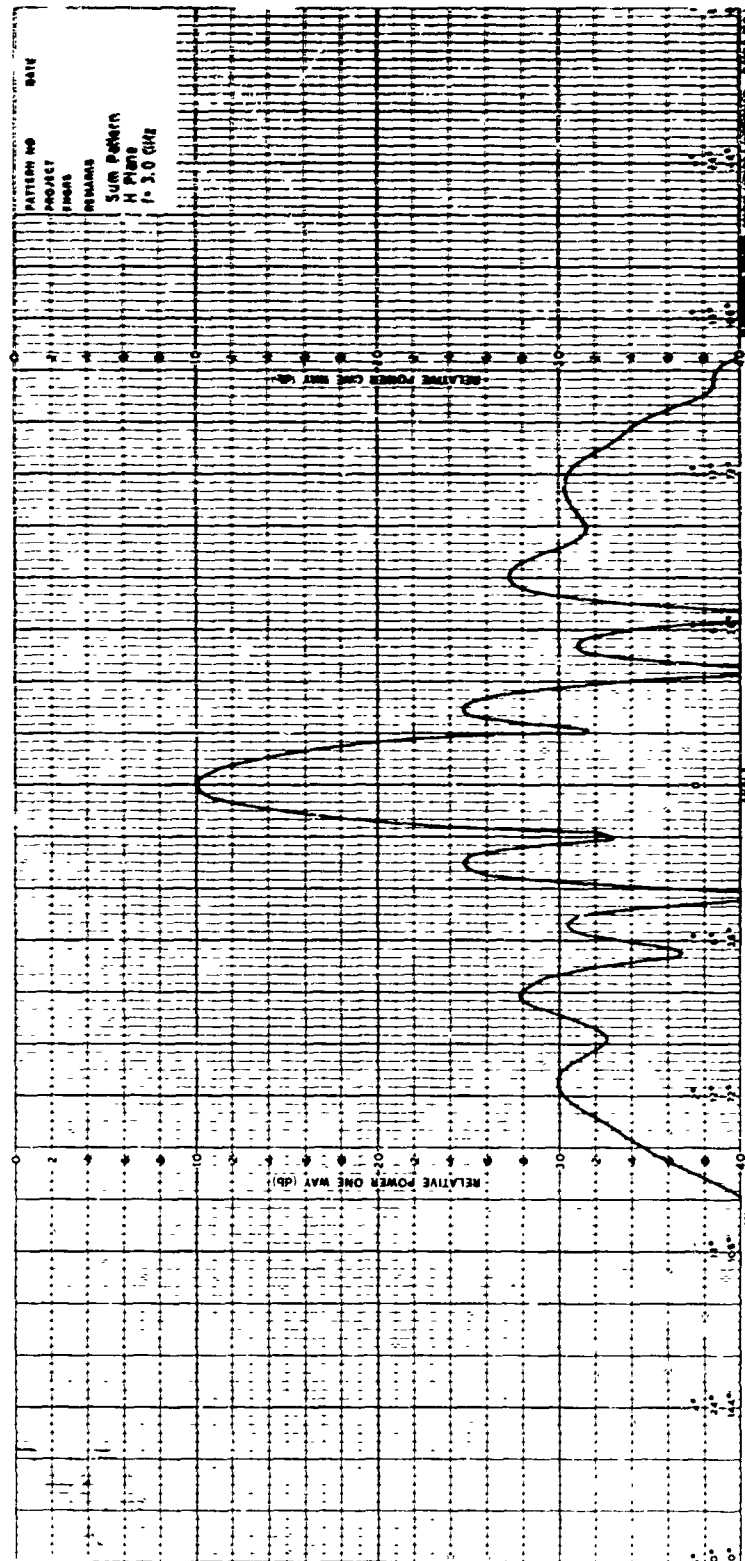


Figure 16. Radiation Pattern of Sixteen-Element SBF Array at  $f = 3.0$  GHz (H plane)

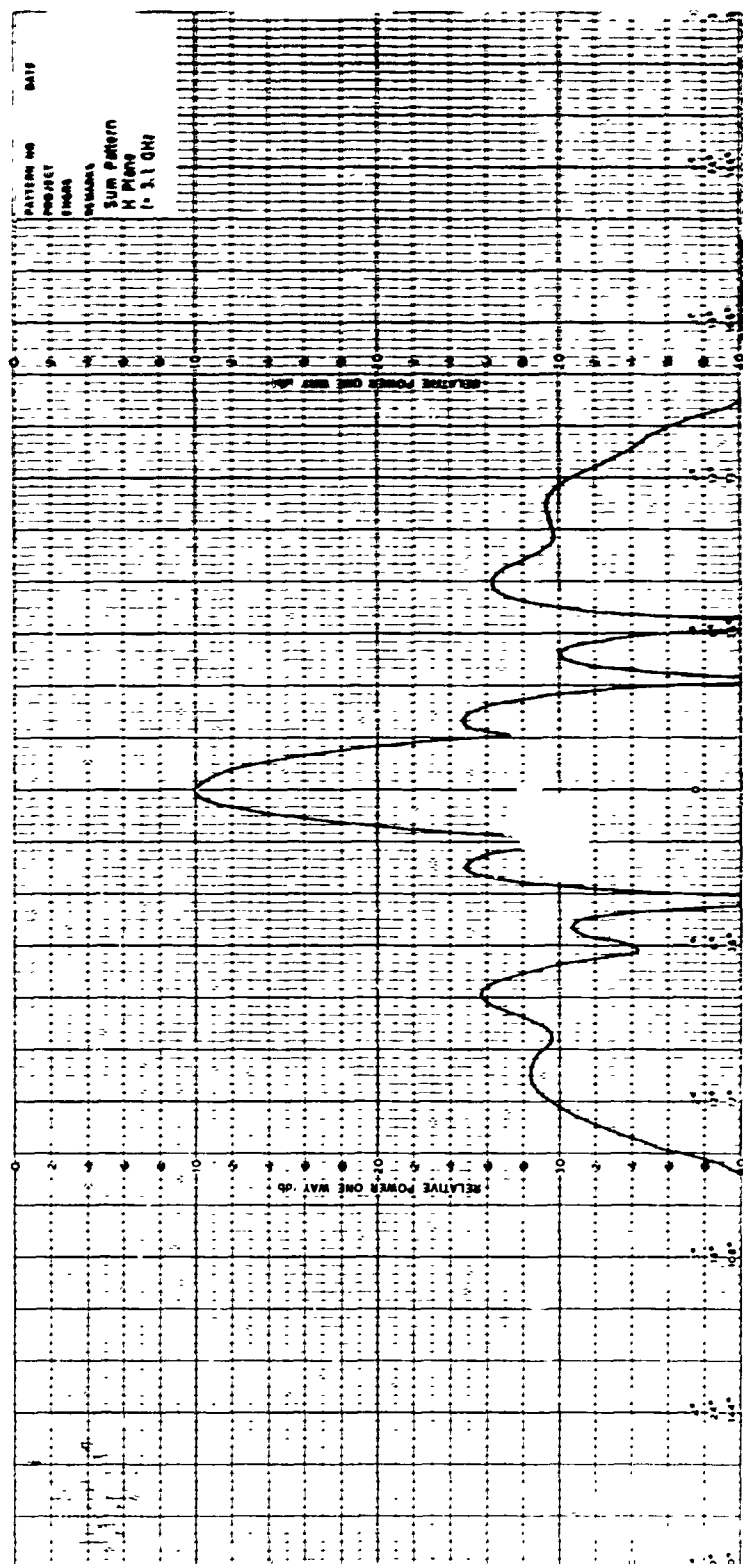
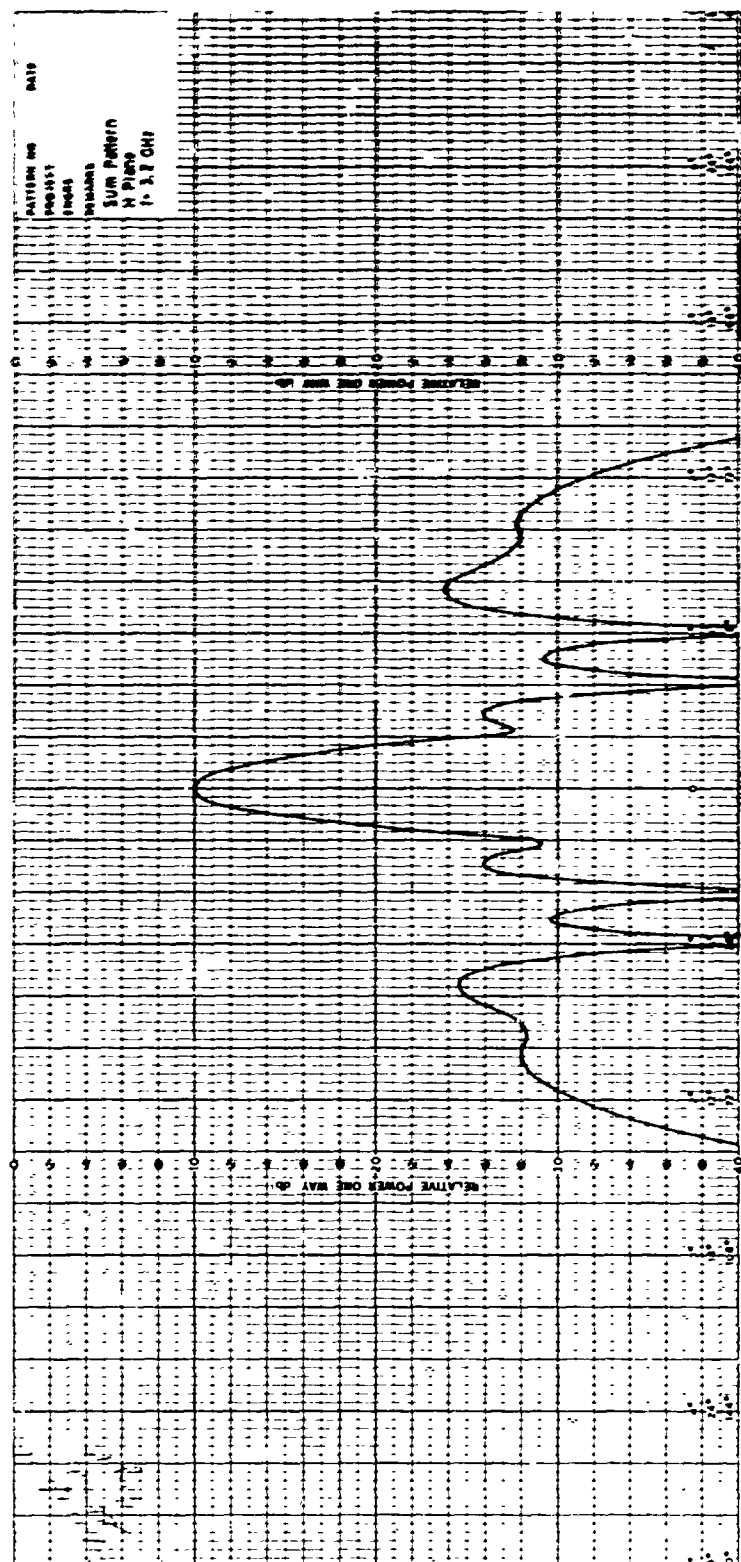


Figure 17. Radiation Pattern of Sixteen-Element SBP Array at  $f = 3.1$  GHz (H plane)





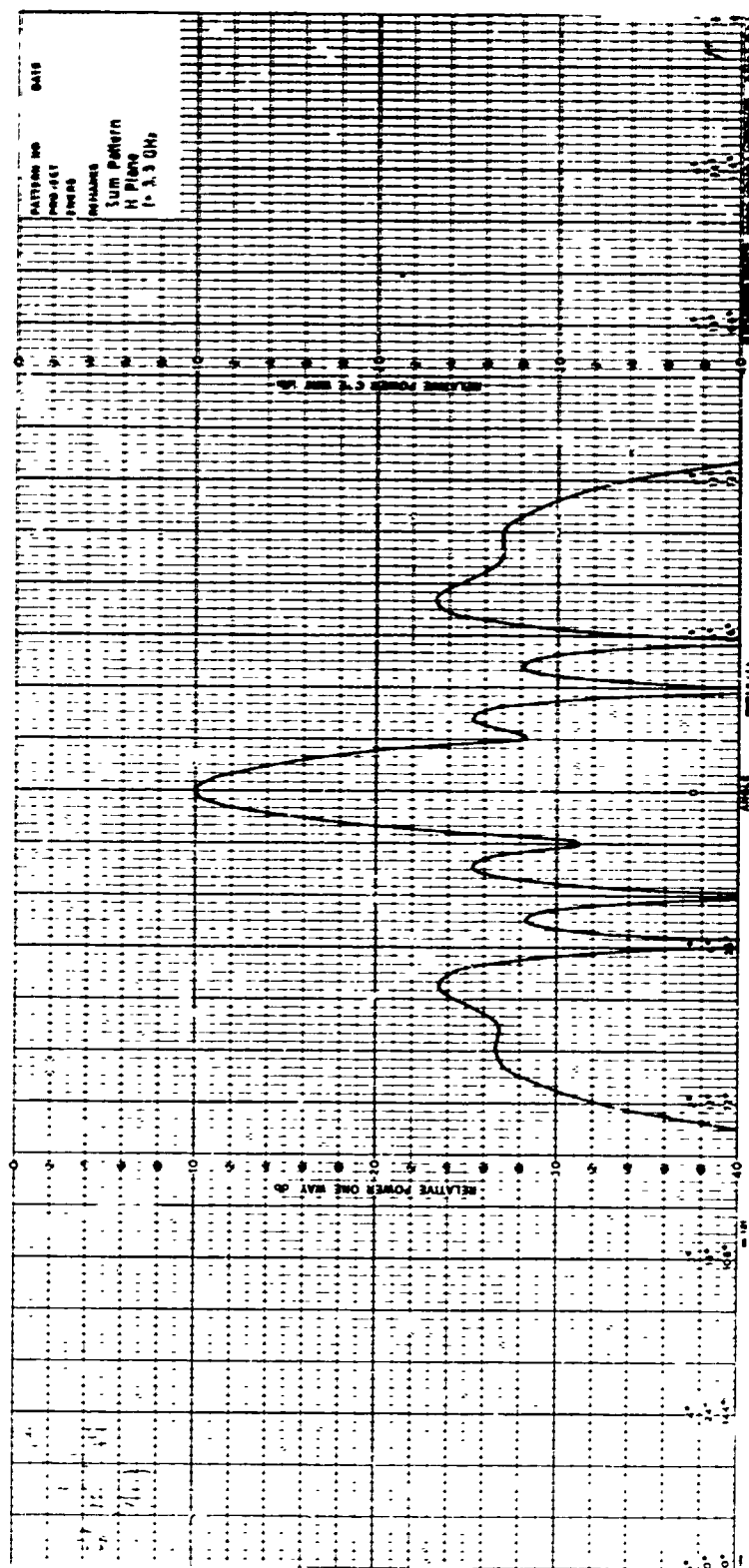


Figure 19. Radiation Pattern of Sixteen-Element SBF Array at  $f = 3.3$  GHz (H plane)

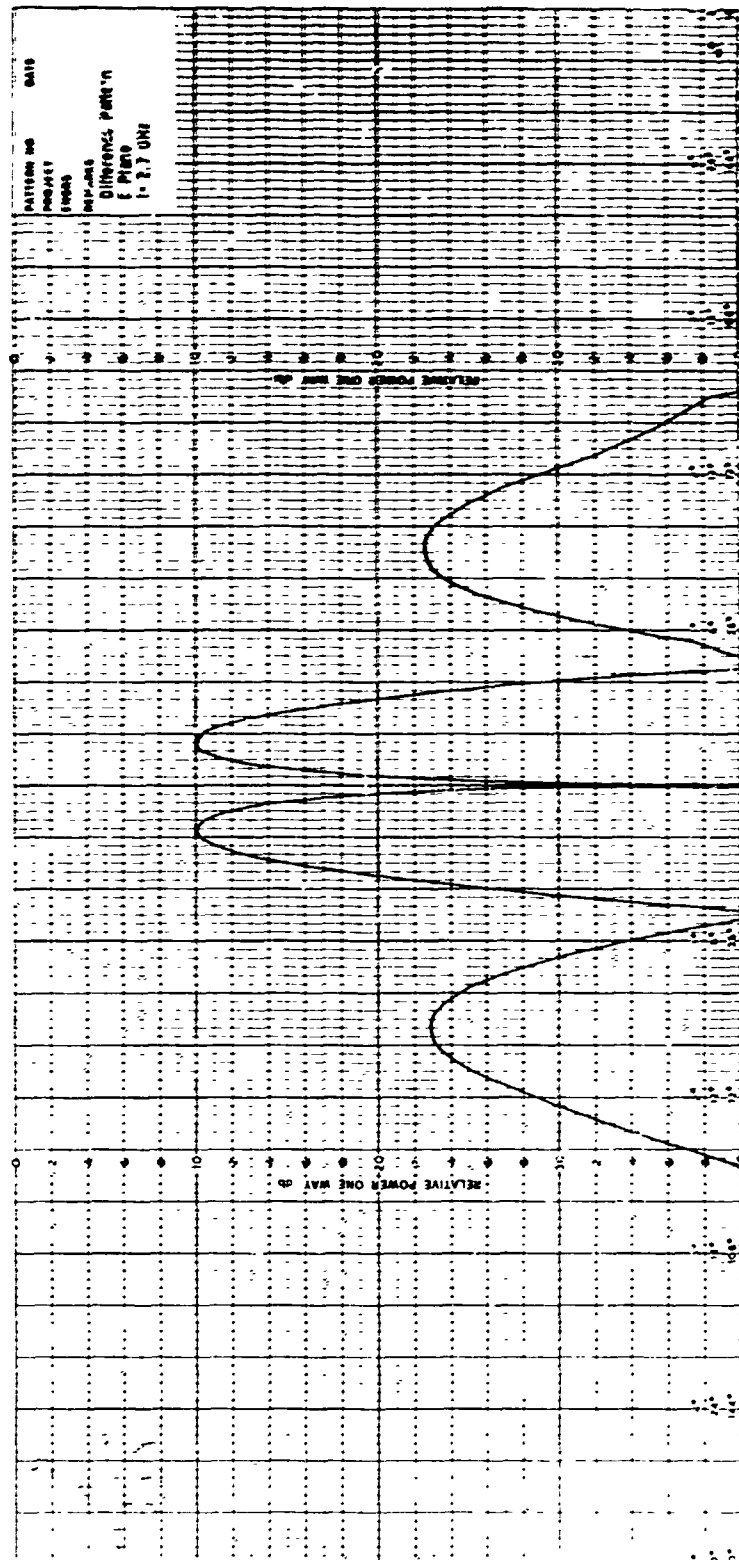


Figure 20. Difference Pattern of Sixteen-Element SSBF Array at  $f = 2.7$  GHz (E plane)

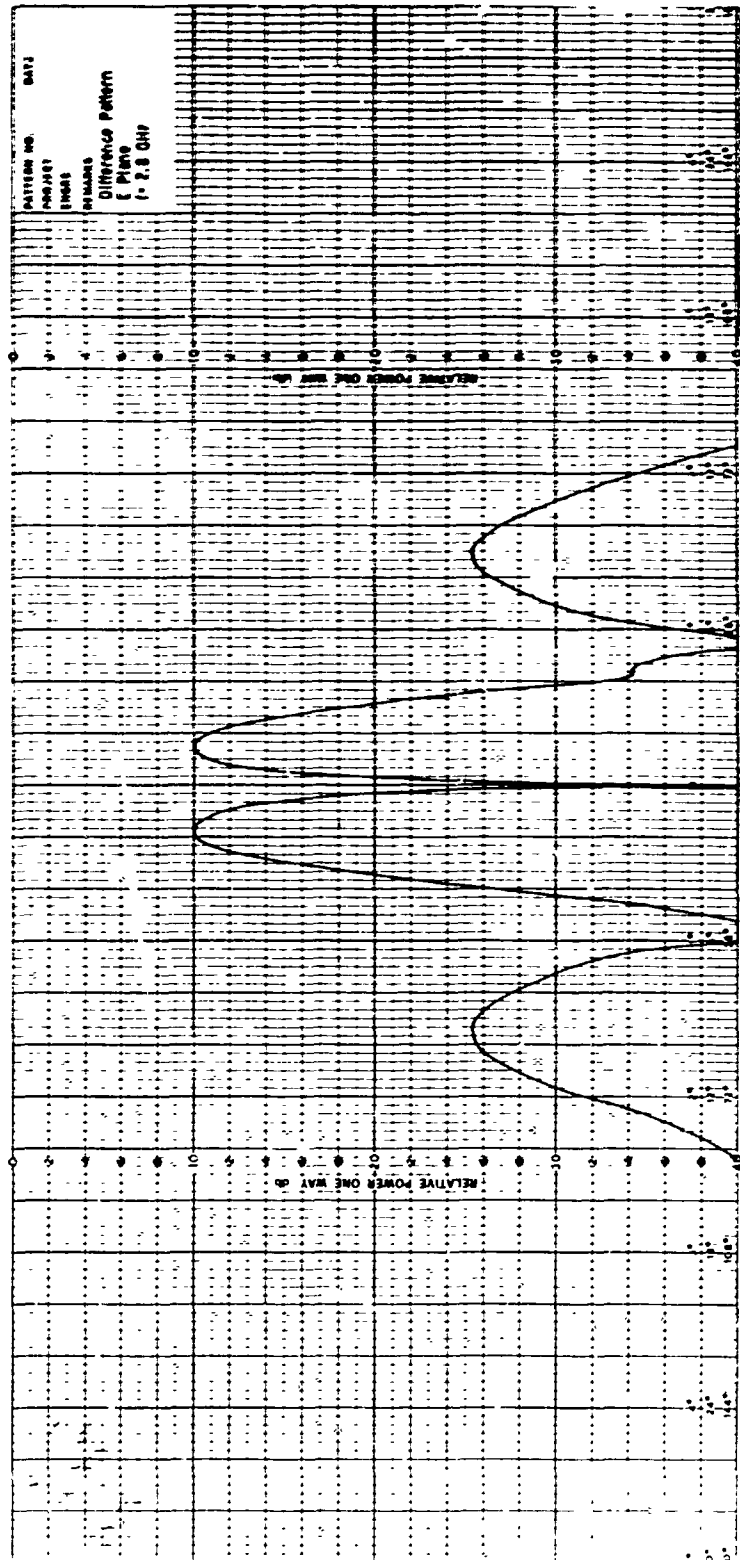


Figure 21. Difference Pattern of Sixteen-Element SBF Array at  $f = 2.8$  GHz (E plane)

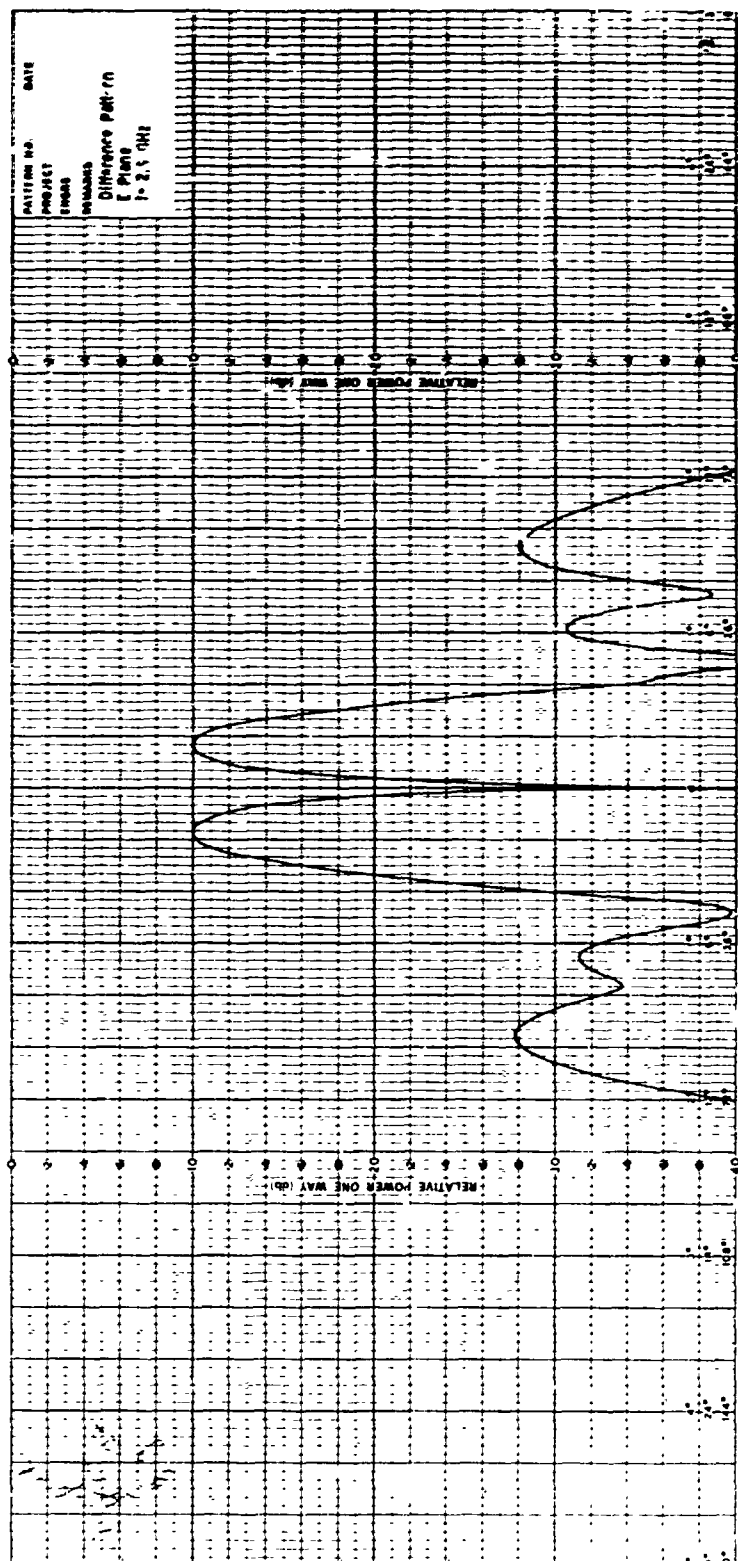


Figure 22. Difference Pattern of Sixteen-Element SHF Array at  $f = 2.9$  GHz (E plane)

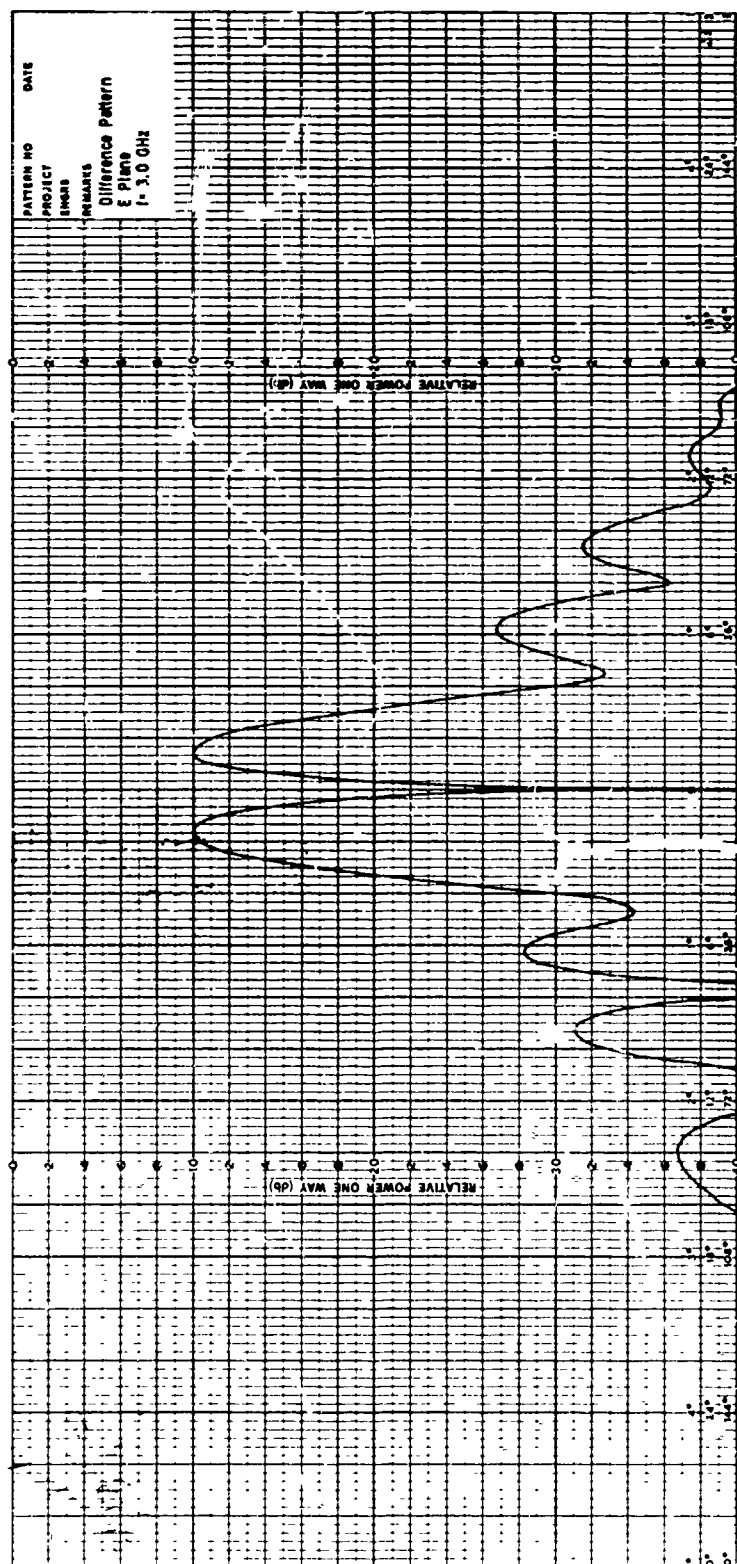


Figure 23. Difference Pattern of Sixteen-Element SBF Array at  $f = 3.0$  GHz (E plane)

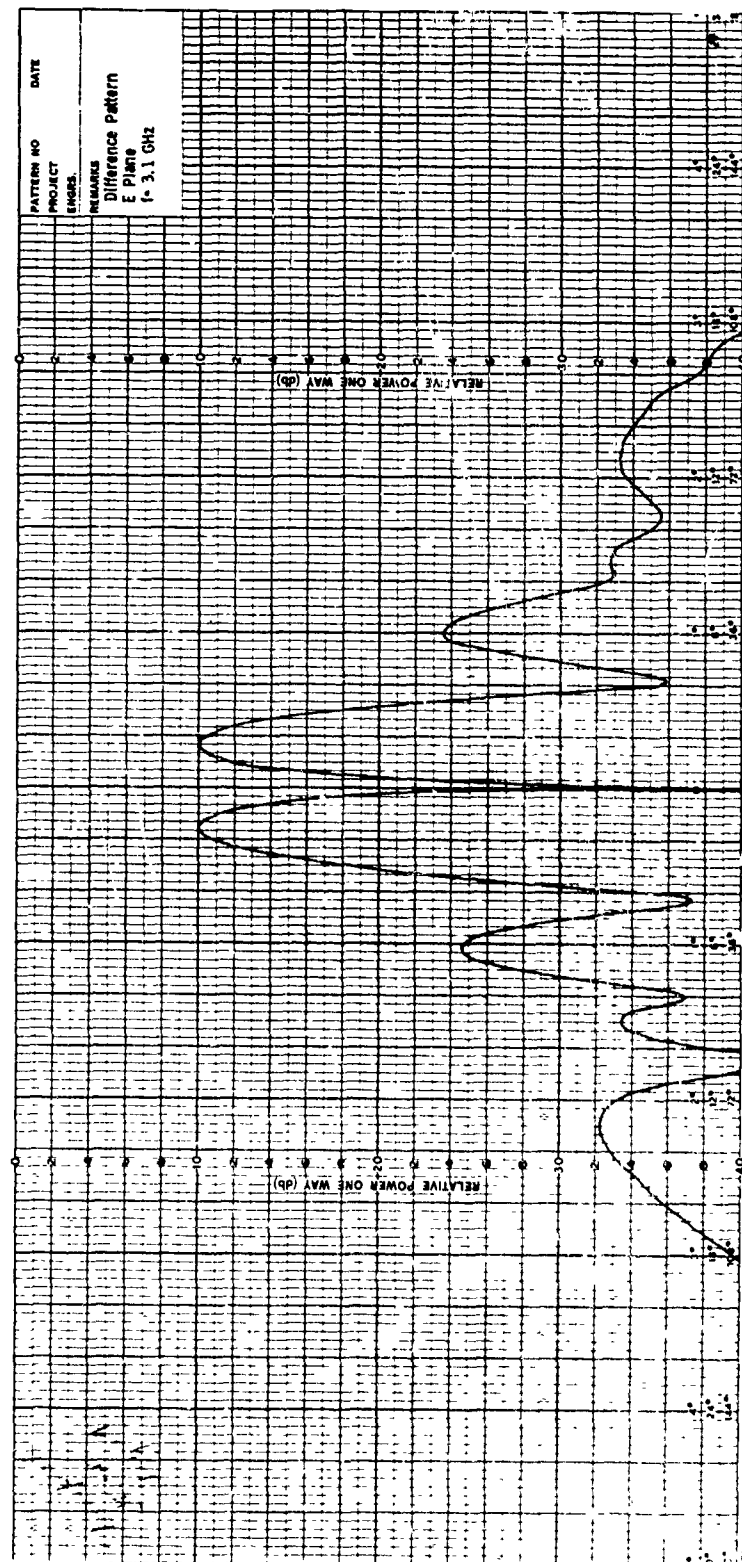


Figure 24. Difference Pattern of Sixteen-Element SBF Array at  $f = 3.1$  GHz (E plane)

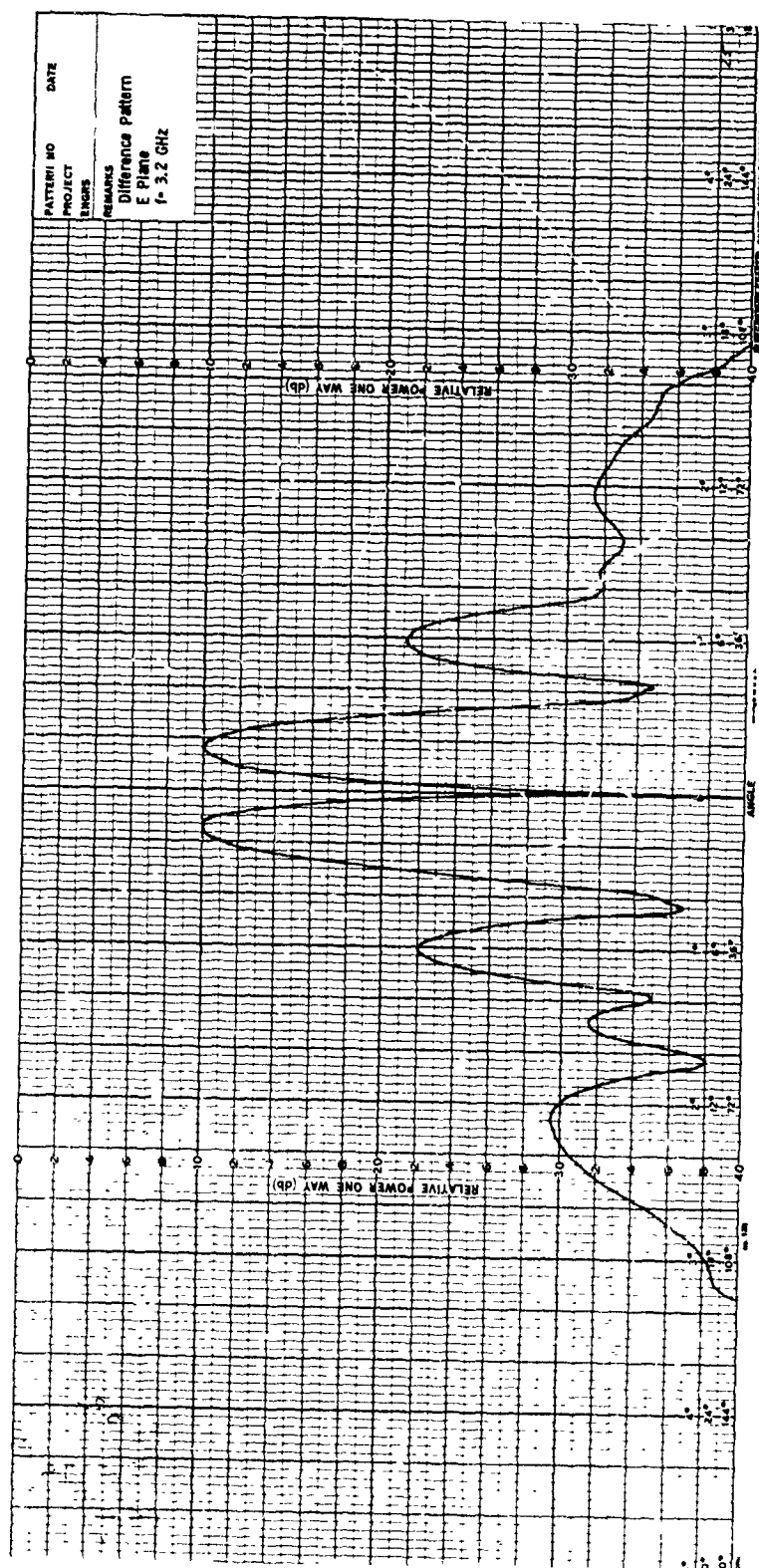
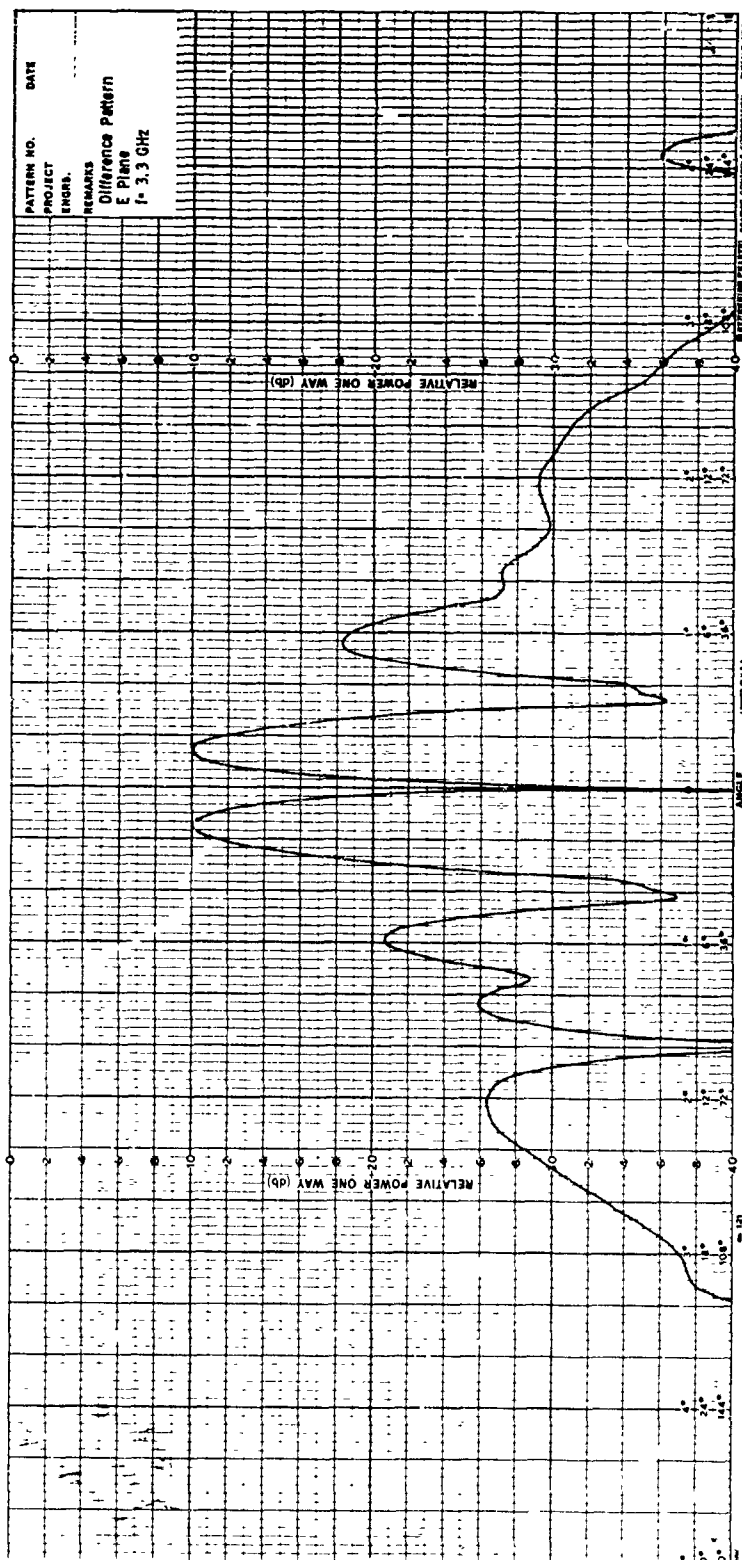


Figure 25. Difference Pattern of Sixteen-Element SBF Array at  $f = 3.2$  GHz (E plane)





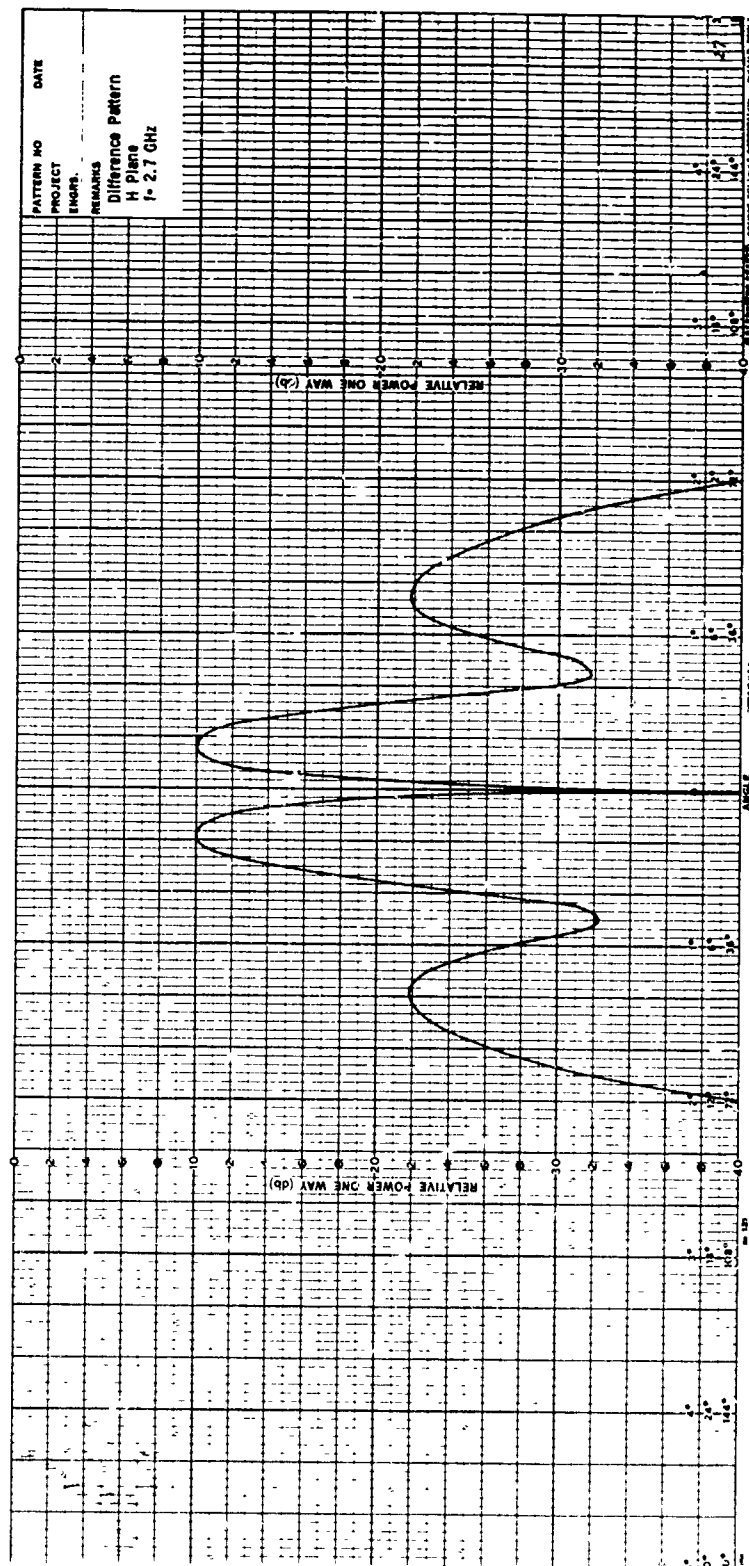


Figure 27. Difference Pattern of Sixteen-Element SBF Array at  $f = 2.7$  GHz (H plane)

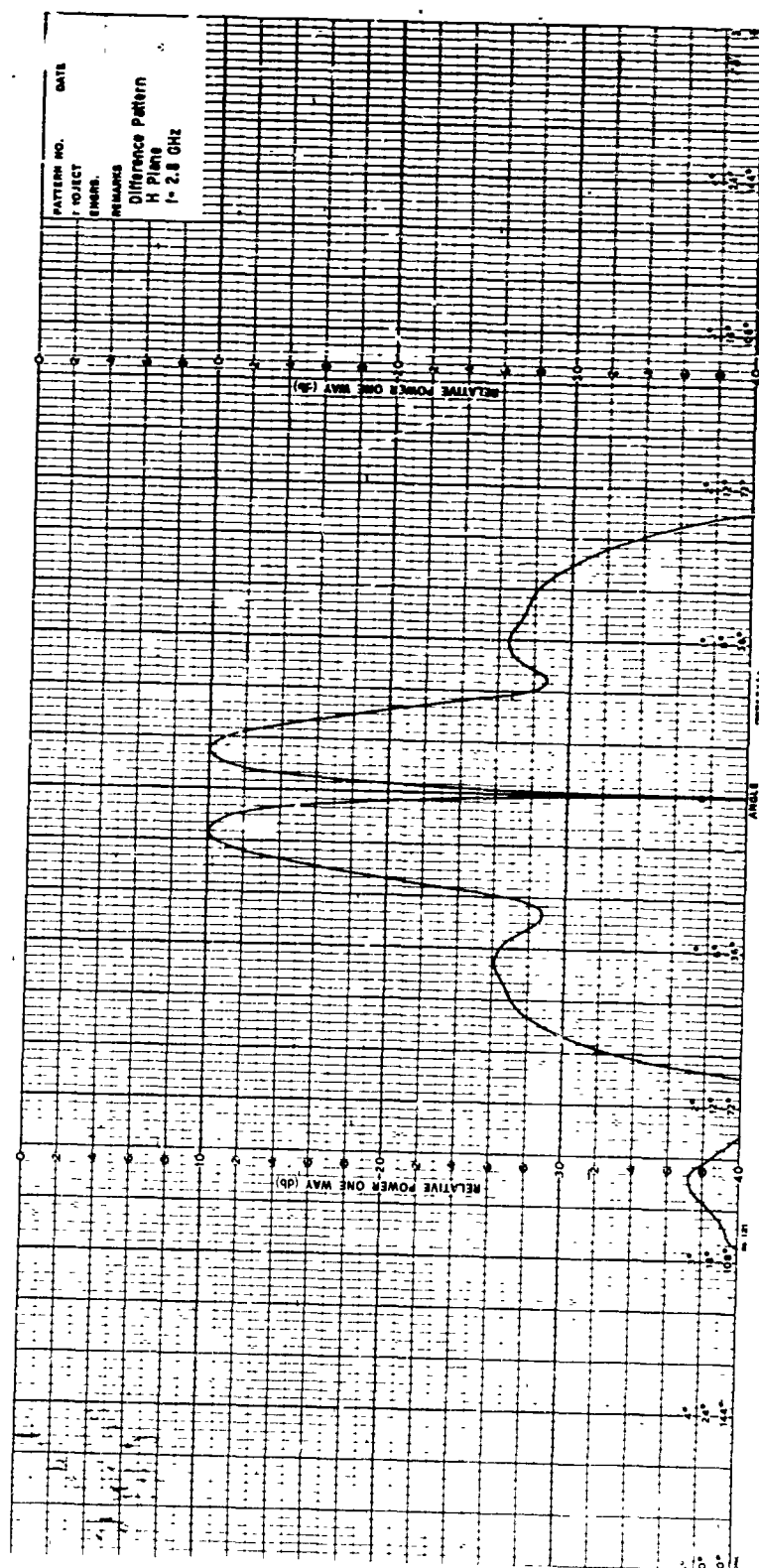


Figure 28. Difference Pattern of Sixteen-Element SBF Array at  $f = 2.8 \text{ GHz}$  (H plane)

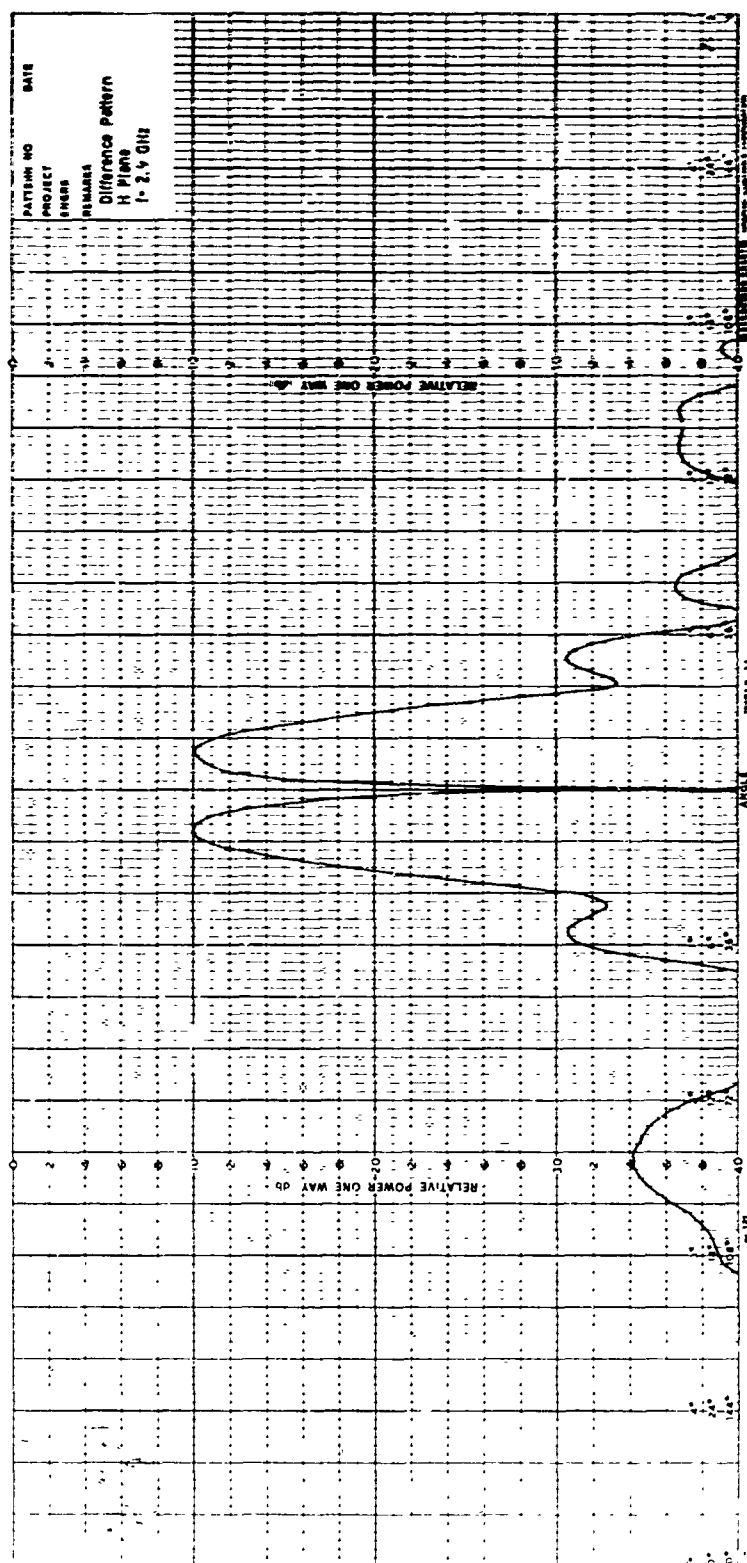


Figure 29. Difference Pattern of Sixteen-Element SHF Array at  $f = 2.9$  GHz (H plane)

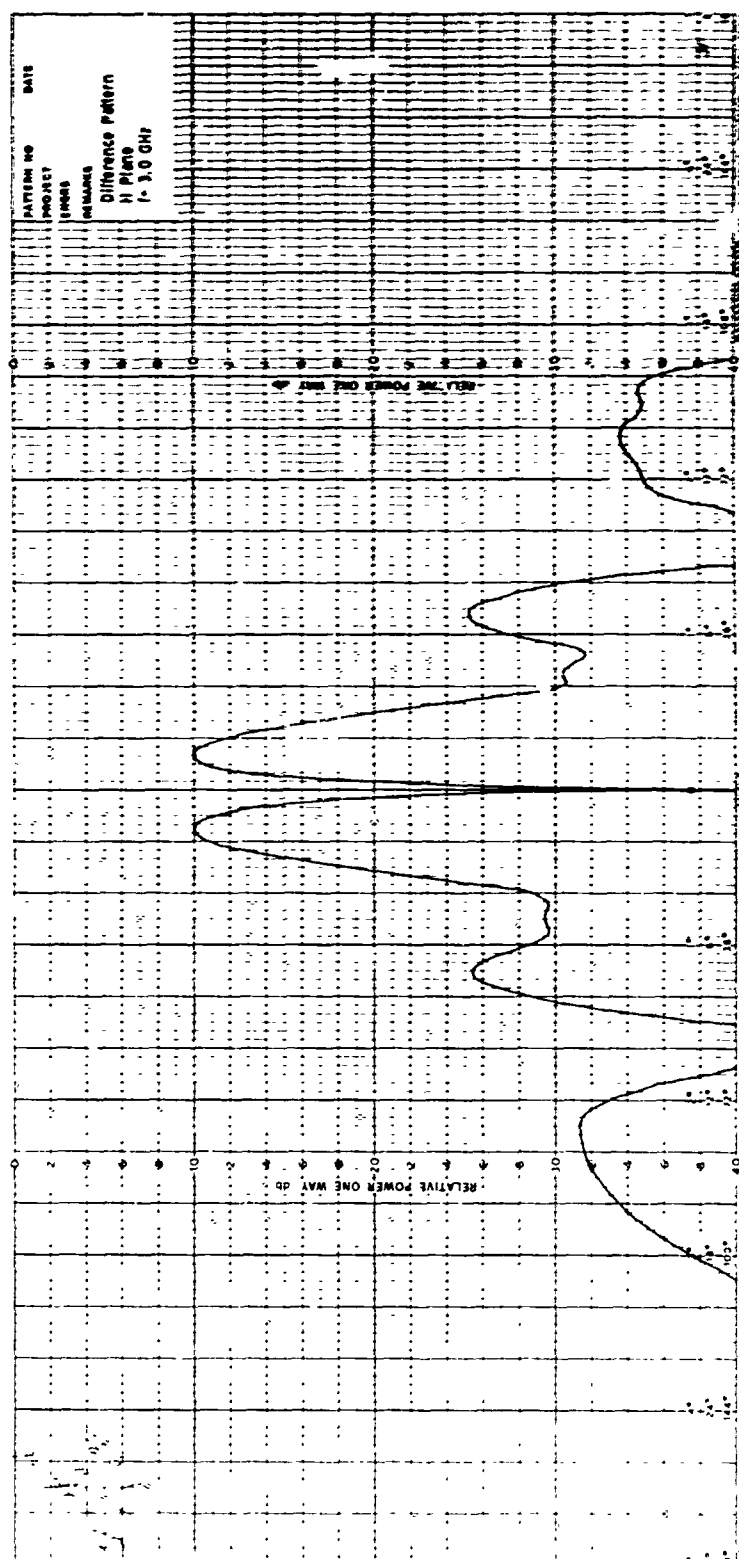


Figure 30. Difference Pattern of Sixteen-Element SHF Array at  $f = 3.0$  GHz (H plane)

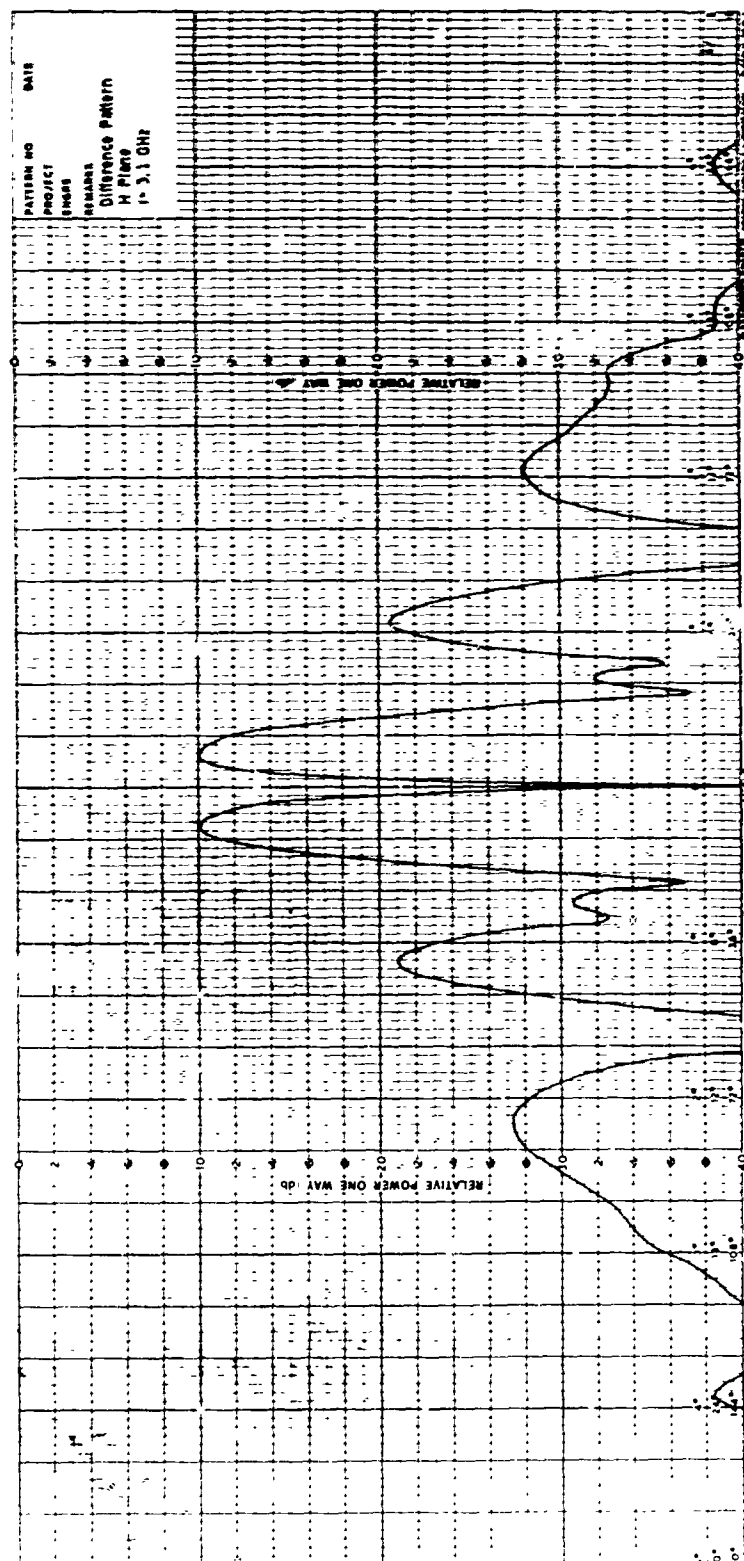


Figure 31. Difference Pattern of Sixteen-Element SBF Array at  $f = 3.1$  GHz (H plane)

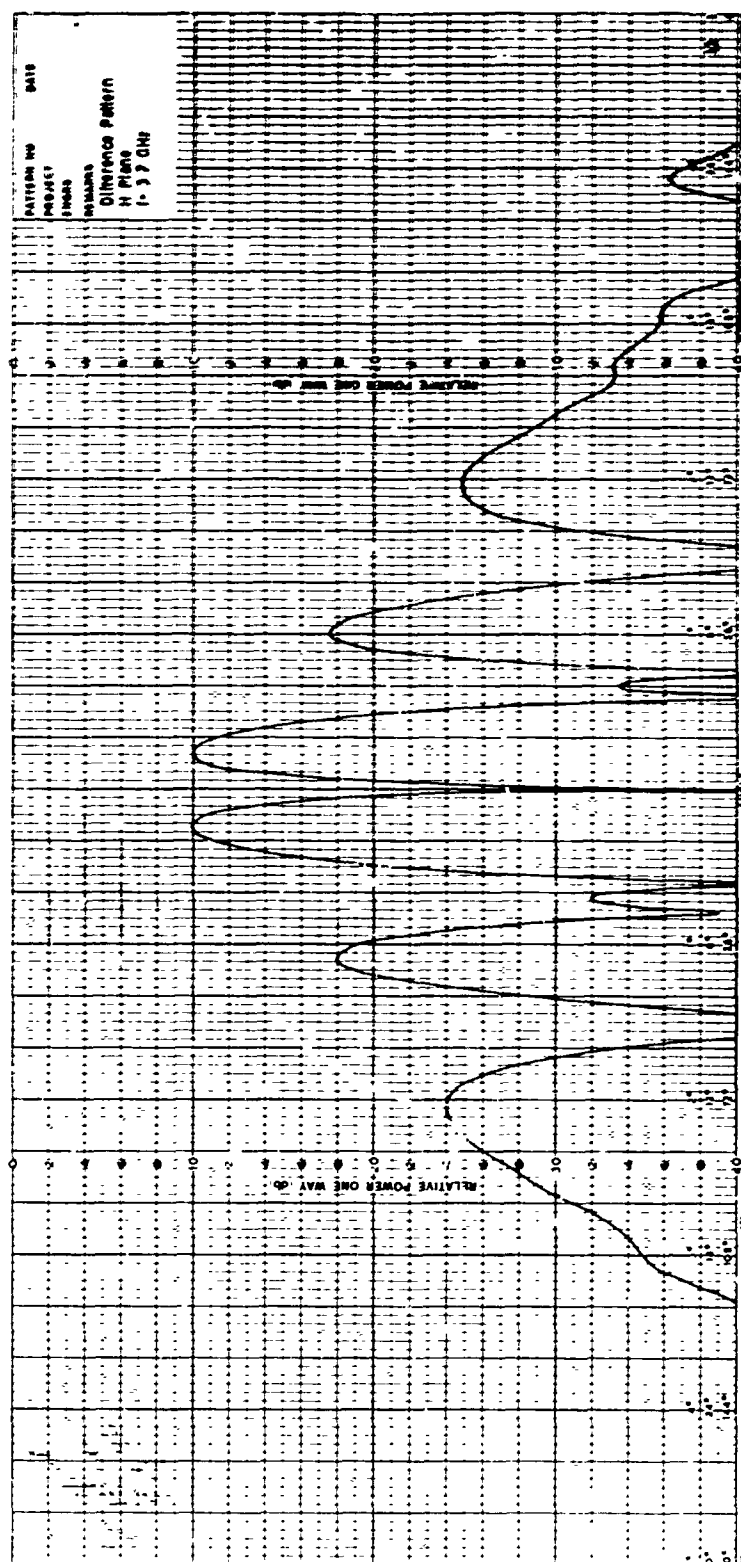


Figure 32. Difference Pattern of Sixteen-Element SHF Array at  $f = 3.2$  GHz (H plane)

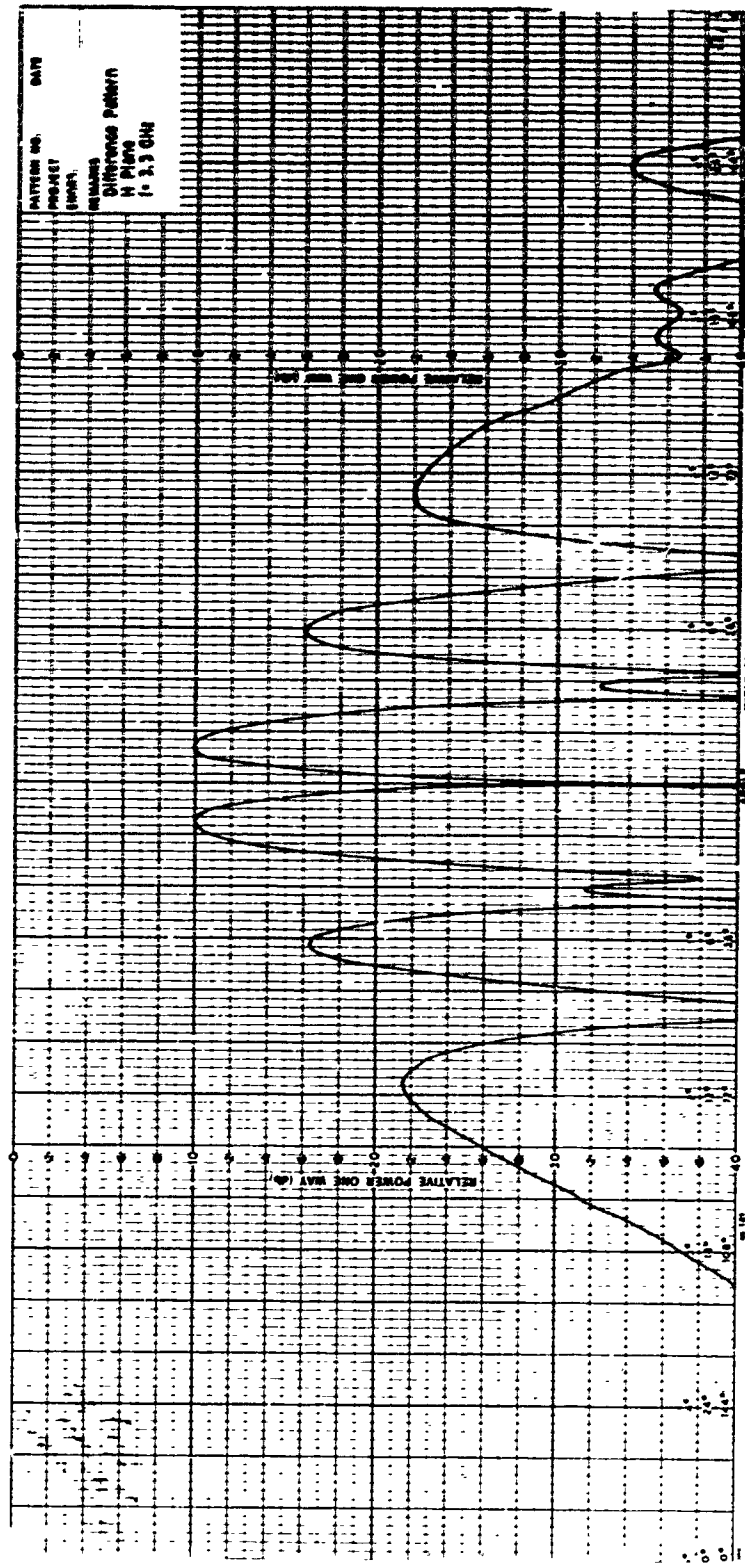


Figure 33. Difference Pattern of Sixteen-Element SBF Array at  $f = 3.3 \text{ GHz}$  (H plane)



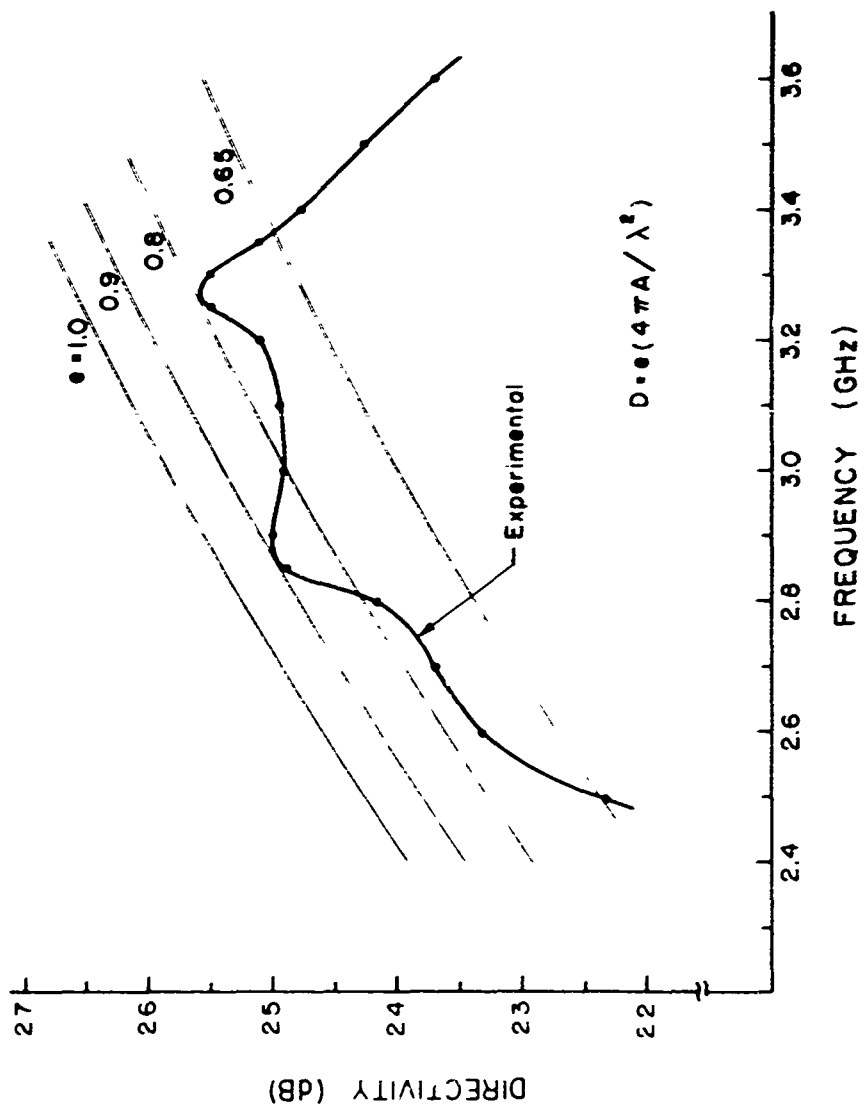


Figure 34. Experimental Curve of Directivity of the Sixteen-Element SPP Array as a Function of Frequency

## References

- Ehrenspeck, H. W. (1965) The Short-Backfire Antenna, Proc. IEEE, 53:1138-1140.
- Ehrenspeck, H. W. (1969) Short-Backfire Antenna, U. S. Patent No. 3438043, April 1969.
- Ehrenspeck, H. W. (1970) Short-Backfire Antenna, U. S. Patent No. 3508278, April 1970.
- Ehrenspeck, H. W., and Strom, J. A. (1971a) The Short-Backfire Antenna as an Element for High-Gain Arrays, AFCRL-71-0234.
- Ehrenspeck, H. W., and Strom, J. A. (1971b) Short-Backfire Arrays, AFCRL-71-0368.
- Ehrenspeck, H. W., and Strom, J. A. (1971c) The Four-Element SBF Array: Variation of Parameters for Optimization of Performance, AFCRL-71-0559.
- Fulmer, M. R., and Moseley, R. E. (1960) Determination of antenna directivity by pattern integration method, The Essay (No. 2), Scientific Atlanta, Inc.
- Oetli, H., and Thomanek, L. (1958) Monopuls-Antenne der Bodenstation für Satellitenfunk der Deutschen Versuchsanstalt für Luft und Raumfahrt e V, NTZ-Nachricht. Z. 21 (Nr. 10):631-634.
- Stegen, R. J. (1964) The gain-beamwidth product of an antenna, IEEE Tr. Antennas and Propagation, AP-12 (No. 4):505-506.

Preceding page blank

## Appendix A

### Description of the Slot Dipoles Used as Feed Elements in the 3-GHz Array Models

In the previous reports on backfire antennas and arrays (Ehrenspeck and Strom, 1971 a, b, c), little information has been given about the structure and input impedance of the slotted dipole and the feeding mechanism of the short-backfire feed element. It has been established, however, that for best operation the dipole should be located approximately midway between the large planar reflector M and the smaller disk reflector R. This geometry creates a high standing-wave field distribution in the cavity space between the reflectors M and R, with its maximum field amplitude at the location of the dipole feed. This effect substantially increases the input impedance at the terminals of the dipole.

Normally, slot dipoles are constructed as terminations on a 50-ohm air coaxial line. Impedance-matching can be accomplished by slight adjustments in the length of the half-wavelength dipole. In the case of the SBF element, however, the impedance is increased to a value of approximately 175 ohms and so this method cannot be used because of the unfavorable mismatch at the 50-ohm terminal.

The approach taken to provide a simple method of impedance compensation is illustrated in Figure A1. This view exposes the center conductor of the 50-ohm air line and the dipole input terminals. The impedance transformation is accomplished by undercutting that portion of the center conductor that immediately precedes the dipole terminals in the form of a coaxial line

Preceding page blank

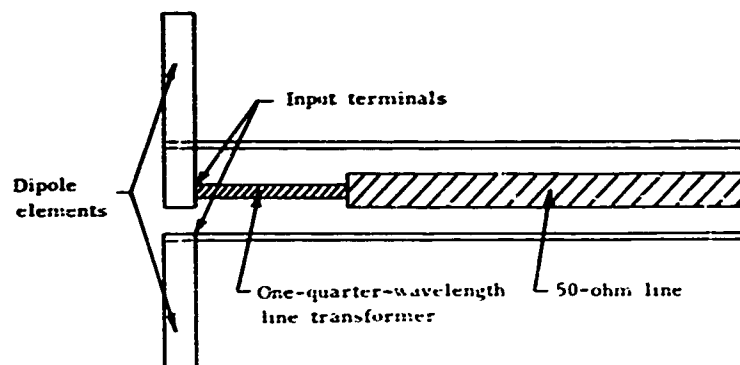


**Figure A1. Sketch of Cross-Sectional View of Slot Dipole and Matching Section of SBF Element**

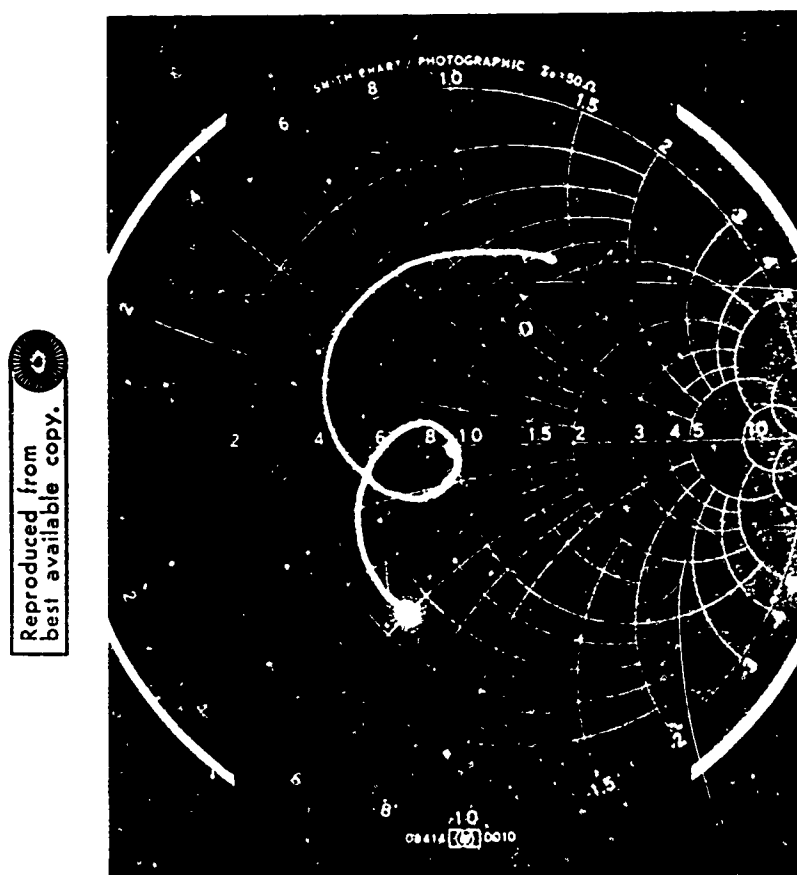


Figure A2. Smith Chart Plot of Matching Curve of the SBF Element in an SBF Array

transformer. With a length of this section made one-quarter wavelength at the frequency of interest, its characteristic impedance  $Z$  for best matching may be calculated according to the equation  $Z = \sqrt{Z_1 Z_2}$ , with  $Z_1$  the characteristic impedance of the transmission line and  $Z_2$  the input impedance of the feed dipole. For our application,  $Z_1 = 50$  ohms,  $Z_2 = 176$  ohms, and  $Z = 93.8$  ohms. The length of the quarter-wavelength section is 2.5 cm for the 3 GHz design frequency.

A typical Smith Chart impedance representation of a single SBF element in an SBF array is shown in Figure A2 for the frequency range 2.9 to 3.1 GHz. Its VSWR reaches 1.0 at the design frequency (3.0 GHz).

Slot dipoles are well suited as feeds for linearly polarized SBF antennas and arrays at frequencies below 1 GHz. If cross- or circular-polarization response is a criterion, sleeve dipoles are more advantageous. They have been used in several applications (Ehrenspeck and Strom, 1971c). At the higher frequencies, close tolerances in construction of slot dipoles must be maintained to ensure array uniformity. Power requirements may also be a limiting factor for high-frequency applications. These disadvantages have, however, been overcome by a new type of backfire feed that will be described in a later report.